Inorganic Chemistry

Article

pubs.acs.org/IC

Emissive Behavior, Cytotoxic Activity, Cellular Uptake, and PEGylation Properties of New Luminescent Rhenium(I) Polypyridine Poly(ethylene glycol) Complexes

Alex Wing-Tat Choi, Man-Wai Louie, Steve Po-Yam Li, Hua-Wei Liu, Bruce Ting-Ngok Chan, Tonlex Chun-Ying Lam, Alex Chun-Chi Lin, Shuk-Han Cheng,* and Kenneth Kam-Wing Lo*

Department of Biology and Chemistry, City University of Hong Kong, Tat Chee Avenue, Kowloon, Hong Kong, P.R. China

Supporting Information

ABSTRACT: We report here a new class of biological reagents derived from luminescent rhenium(I) polypyridine complexes modified with a poly(ethylene glycol) (PEG) pendant. The PEG-amine complexes $[Re(N^\wedge N)(CO)_3(py\text{-}PEG\text{-}NH_2)](PF_6)$ (py-PEG-NH_2 = 3-amino-5-(*N*-(2-(*ω*-methoxypoly(1-oxapropyl))ethyl)aminocarbonyl)pyridine, MW_{PEG} = 5000 Da, PDI_{PEG} < 1.08; N^N = 1,10-phenanthroline (phen) (**1-PEG-NH$_2$**), 3,4,7,8-tetramethyl-1,10-phenanthroline (Me_4-phen) (**2-PEG-NH$_2$**), 4,7-diphenyl-1,10-phenanthroline (Ph_2-phen) (**3-PEG-NH$_2$**)) and $[Re(bpy\text{-}PEG)(CO)_3(py\text{-}NH_2)](PF_6)$ (bpy-PEG = 4-(*N*-(2-(*ω*-methoxypoly(1-oxapropyl))ethyl)aminocarbonyl)-4′-methyl-2,2′-bipyridine; py-NH_2 = 3-aminopyridine) (**4-PEG-NH$_2$**) have been synthesized and characterized. The photophysical properties, lipophilicity, water solubility, cytotoxic activity, and cellular uptake properties of these complexes have been compared to those of their PEG-free counterparts $[Re(N^\wedge N)(CO)_3(py\text{-}Et\text{-}NH_2)](PF_6)$ (py-Et-NH_2 = 3-amino-5-(*N*-(ethyl)-aminocarbonyl)pyridine; N^N = phen (**1-Et-NH$_2$**), Me_4-phen (**2-Et-NH$_2$**), Ph_2-phen (**3-Et-NH$_2$**)) and $[Re(bpy\text{-}Et)(CO)_3(py\text{-}NH_2)](PF_6)$ (bpy-Et = 4-(*N*-(ethyl)aminocarbonyl)-4′-methyl-2,2′-bipyridine) (**4-Et-NH$_2$**). The PEG complexes exhibited significantly higher water solubility and lower cytotoxicity (IC_{50} = 6.6 to 1152 *μ*M) than their PEG-free counterparts (IC_{50} = 3.6 to 159 *μ*M), indicating that the covalent attachment of a PEG pendant to rhenium(I) polypyridine complexes is an effective way to increase their biocompatibility. The amine complexes **1-PEG-NH$_2$**–**4-PEG-NH$_2$** have been activated with thiophosgene to yield the isothiocyanate complexes $[Re(N^\wedge N)(CO)_3(py\text{-}PEG\text{-}NCS)](PF_6)$ (py-PEG-NCS = 3-isothiocyanato-5-(*N*-(2-(*ω*-methoxypoly(1-oxapropyl))ethyl)aminocarbonyl)pyridine; N^N = phen (**1-PEG-NCS**), Me_4-phen (**2-PEG-NCS**), Ph_2-phen (**3-PEG-NCS**)), and $[Re(bpy\text{-}PEG)(CO)_3(py\text{-}NCS)](PF_6)$ (py-NCS = 3-isothiocyanatopyridine) (**4-PEG-NCS**) as a new class of luminescent PEGylation reagents. To examine their PEGylation properties, these isothiocyanate complexes have been reacted with a model substrate *n*-butylamine, resulting in the formation of the thiourea complexes $[Re(N^\wedge N)(CO)_3(py\text{-}PEG\text{-}Bu)](PF_6)$ (py-PEG-Bu = 3-*n*-butylthioureidyl-5-(*N*-(2-(*ω*-methoxypoly(1-oxapropyl))ethyl)aminocarbonyl)pyridine; N^N = phen (**1-PEG-Bu**), Me_4-phen (**2-PEG-Bu**), Ph_2-phen (**3-PEG-Bu**)), and $[Re(bpy\text{-}PEG)(CO)_3(py\text{-}Bu)](PF_6)$ (py-Bu = 3-*n*-butylthioureidylpyridine) (**4-PEG-Bu**). Additionally, bovine serum albumin (BSA) and poly(ethyleneimine) (PEI) have been PEGylated with the isothiocyanate complexes to yield bioconjugates **1-PEG-BSA**–**4-PEG-BSA** and **1-PEG-PEI**–**4-PEG-PEI**, respectively. Upon irradiation, all the PEGylated BSA and PEI conjugates exhibited intense and long-lived emission in aqueous buffer under ambient conditions. The DNA-binding and polyplex-formation properties of conjugate **3-PEG-PEI** have been studied and compared with those of unmodified PEI. Furthermore, the in vivo toxicity of complex **3-PEG-NH$_2$** and its PEG-free counterpart **3-Et-NH$_2$** has been investigated using zebrafish embryos as an animal model. Embryos treated with the PEG complex at high concentrations revealed delayed hatching, which has been ascribed to hypoxia as a result of adhering of the complex to the external surface of the chorion.

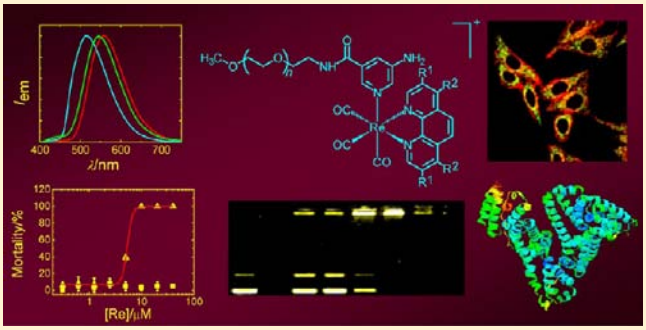

INTRODUCTION

PEGylation is a covalent modification of proteins, peptides, antibody fragments, and drug molecules with poly(ethylene glycol) (PEG). This derivatization procedure significantly reduces the toxicity of the molecules without sacrificing their specific biological or therapeutic properties.[1] PEGylated molecules show reduced aggregation tendency and nonspecific interactions with surfaces and other biological entities and display enhanced biodistribution, pharmacokinetics, and resistance to undesirable proteolysis.[2] Additionally, PEG has been used as a highly flexible spacer-arm for protein-

Received: September 6, 2012
Published: November 30, 2012

   dx.doi.org/10.1021/ic301948d | *Inorg. Chem.* 2012, 51, 13289–13302

Chart 1. Structures of Complexes 1-PEG-NH_2−4-PEG-NH_2, 1-Et-NH_2−4-Et-NH_2, 1-PEG-NCS−4-PEG-NCS, and 1-PEG-Bu−4-PEG-Bu

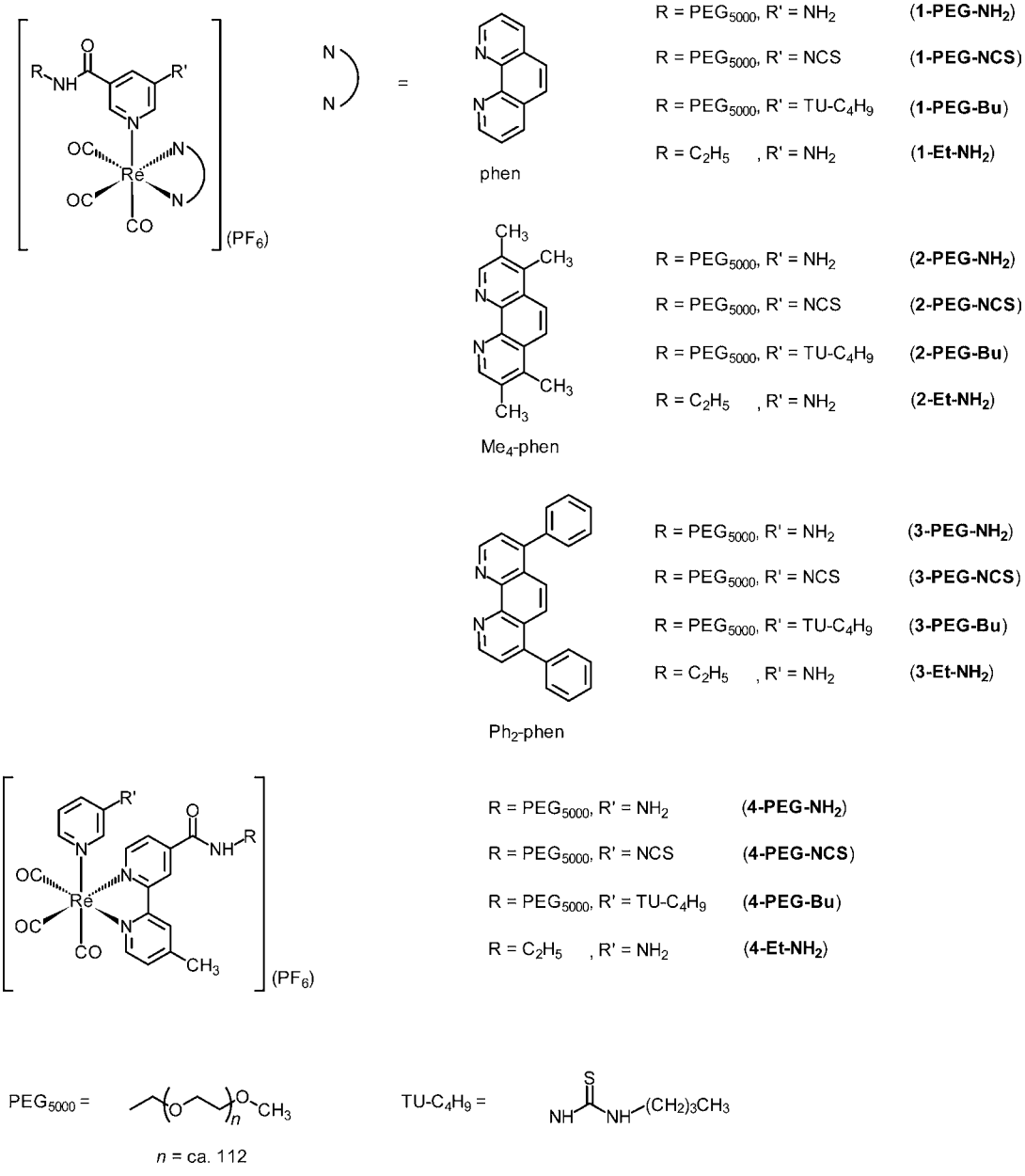

conjugation[3] and protein-cross-linking.[4] Since PEGylation is such a useful bioconjugation process, PEGylation reagents with a wide range of molecular weights and shapes, reactive functional groups for modification, and specific properties have been developed.[5] Those reagents containing fluorescent units such as the dansyl group,[6] BODIPY,[7] and fluorescein[8] are particularly useful in the modification of biological targets as they not only confer the aforementioned properties but also enable detection and quantitation of the targets by optical methods.

In fact, transition metal complexes have been modified with PEG to increase their aqueous solubility; for example, there is a growing interest in using transition metal PEG complexes as soluble polymer-supported catalysts.[9] Also, reports on the electro-optical applications of transition metal PEG complexes with intriguing emission properties have appeared.[10] In addition to the work on the modification of cisplatin with PEG and the incorporation of related anticancer drugs into PEG-containing micelles,[11] there is an emerging interest in the use of transition metal PEG complexes in biological applications; for example, the luminescent platinum(II) complex [Pt(C^N^N-4-Ph-PEGm)]Cl has been designed as a sensitive light-switch for proteins.[12] G3- and G4-poly(amidoamine) (PAMAM) dendrimers have also been modified with organorhenium $CpRe(CO)_3$ units and PEG chains, yielding immunological reagents for carbonyl metalloimmunoassays.[13] Additionally, folic acid has been conjugated to a tricarbonylrhenium(I) unit with a PEG linker to examine its receptor-mediated endocytotic uptake by A2780/AD cells.[14]

Despite these studies, the biological applications of luminescent transition metal PEG complexes are still relatively unexplored. Recently, we have reported a new class of luminescent iridium(III) polypyridine PEG complexes that possess high water solubility and low cytotoxicity as new

dx.doi.org/10.1021/ic301948d | Inorg. Chem. 2012, 51, 13289−13302

Table 1. Photophysical Data of Complexes 1-PEG-NH_2−4-PEG-NH_2, 1-Et-NH_2−4-Et-NH_2, 1-PEG-NCS−4-PEG-NCS, and 1-PEG-Bu−4-PEG-Bu

complex	medium (T/K)	λ_{em}/nm	τ_o/μs	Φ_{em}	k_r/s^{-1}	k_{nr}/s^{-1}
1-PEG-NH_2	CH_2Cl_2 (298)	532	2.18	0.11	5.1×10^4	4.1×10^5
	CH_3CN (298)	546	0.73	0.048	4.1×10^4	1.3×10^6
	buffer (298)[a]	543	0.14	0.018	1.3×10^5	7.0×10^6
	glass (77)[b]	508	10.13			
2-PEG-NH_2	CH_2Cl_2 (298)	491 sh, 511	16.05	0.29	1.8×10^4	4.4×10^4
	CH_3CN (298)	487 sh, 516	12.9	0.22	1.7×10^4	6.1×10^4
	buffer (298)[a]	487 sh, 512	0.85	0.013	1.5×10^4	1.2×10^5
	glass (77)[b]	468 (max), 502, 539 sh	42.71 (22%), 150.57 (78%)			
3-PEG-NH_2	CH_2Cl_2 (298)	545	6.24	0.26	4.2×10^4	1.2×10^5
	CH_3CN (298)	559	2.32	0.061	2.6×10^4	4.1×10^5
	buffer (298)[a]	563	0.61	0.026	4.3×10^4	1.6×10^6
	glass (77)[b]	511, 540 sh	19.50			
4-PEG-NH_2	CH_2Cl_2 (298)	552	0.45	0.010	2.2×10^4	2.2×10^6
	CH_3CN (298)	578	0.21	0.0041	2.0×10^4	4.7×10^6
	buffer (298)[a]	580	0.07	0.0019	2.7×10^4	1.4×10^7
	glass (77)[b]	517	5.24			
1-Et-NH_2	CH_2Cl_2 (298)	530	2.65	0.30	1.1×10^5	2.6×10^5
	CH_3CN (298)	547	1.26	0.18	1.4×10^5	6.5×10^5
	buffer (298)[c]	544	0.07	0.010	1.4×10^5	1.4×10^7
	glass (77)[b]	502	11.19			
2-Et-NH_2	CH_2Cl_2 (298)	488 sh, 512	11.33	0.44	3.9×10^4	4.9×10^4
	CH_3CN (298)	486 sh, 514	9.16	0.28	3.1×10^4	7.9×10^4
	buffer (298)[c]	486 sh, 513	0.62	0.0087	1.4×10^4	1.6×10^6
	glass (77)[b]	467(max), 501, 539 sh	41.92 (22%), 152.17 (78%)			
3-Et-NH_2	CH_2Cl_2 (298)	545	8.00	0.33	4.1×10^4	8.4×10^4
	CH_3CN (298)	559	3.97	0.20	5.0×10^4	2.0×10^5
	buffer (298)[c]	558	0.42	0.021	5.0×10^4	2.3×10^6
	glass (77)[b]	510, 533 sh	20.49			
4-Et-NH_2	CH_2Cl_2 (298)	547	0.46	0.037	8.0×10^4	2.1×10^6
	CH_3CN (298)	578	0.28	0.013	4.6×10^4	3.5×10^6
	buffer (298)[c]	584	0.02	0.0015	7.5×10^4	5.0×10^7
	glass (77)[b]	521	5.46			
1-PEG-NCS	CH_2Cl_2 (298)	525	2.90	0.26	9.0×10^4	2.6×10^5
	CH_3CN (298)	540	1.88	0.072	3.8×10^4	4.9×10^5
	glass (77)[b]	508	9.42			
2-PEG-NCS	CH_2Cl_2 (298)	486 sh, 507	13.68	0.28	2.1×10^4	5.3×10^4
	CH_3CN (298)	490 sh, 510	12.08	0.14	1.2×10^4	7.1×10^4
	glass (77)[b]	470 (max), 501, 535 sh	30.07 (21%), 111.52 (79%)			
3-PEG-NCS	CH_2Cl_2 (298)	539	9.23	0.29	3.1×10^4	7.7×10^4
	CH_3CN (298)	552	3.79	0.050	1.3×10^4	2.5×10^5
	glass (77)[b]	513, 538 sh	20.36			
4-PEG-NCS	CH_2Cl_2 (298)	552	0.63	0.089	1.4×10^5	1.5×10^6
	CH_3CN (298)	572	0.26	0.0050	1.9×10^4	3.8×10^6
	glass (77)[b]	513	5.99			
1-PEG-Bu	CH_2Cl_2 (298)	527	3.20	0.28	8.8×10^4	2.3×10^5
	CH_3CN (298)	541	1.68	0.056	3.3×10^4	5.6×10^5
	buffer (298)[a]	542	1.19	0.043	3.6×10^4	8.0×10^5
	glass (77)[b]	510	9.76			
2-PEG-Bu	CH_2Cl_2 (298)	486 sh, 511	13.40	0.39	2.9×10^4	4.6×10^4
	CH_3CN (298)	482 sh, 513	9.73	0.18	1.9×10^4	8.4×10^4
	buffer (298)[a]	487 sh, 513	4.21	0.079	1.9×10^4	2.2×10^5
	glass (77)[b]	470 (max), 501, 537 sh	32.48 (18%), 146.15 (82%)			
3-PEG-Bu	CH_2Cl_2 (298)	541	9.20	0.30	3.3×10^4	7.6×10^4
	CH_3CN (298)	554	3.83	0.049	1.3×10^4	2.5×10^5
	buffer (298)[a]	560	2.88	0.045	1.6×10^4	3.3×10^5
	glass (77)[b]	516, 538 sh	19.33			
4-PEG-Bu	CH_2Cl_2 (298)	554	0.53	0.017	3.2×10^4	1.9×10^6
	CH_3CN (298)	575	0.19	0.014	7.4×10^4	5.2×10^6
	buffer (298)[a]	588	0.08	0.0060	7.5×10^4	1.2×10^7
	glass (77)[b]	514	5.92			

dx.doi.org/10.1021/ic301948d | Inorg. Chem. 2012, 51, 13289−13302

Table 1. continued

[a]50 mM potassium phosphate buffer at pH 7.4. [b]In butyronitrile glass. [c]50 mM potassium phosphate buffer at pH 7.4 containing 10% methanol.

bioprobes and imaging reagents.[15] Thus, we envisage that the incorporation of a PEG pendent to rhenium(I) polypyridine complexes would significantly increase their biocompatibility. The advantages of rhenium(I) polypyridine complexes are their ease of emission color-tuning using different diimine ligands and their long-lived excited states, which are useful in the development of multicolor probes for time-resolved applications such as fluorescence lifetime imaging microscopy (FLIM). Additionally, since the coordination chemistry of the group 7 congeners rhenium and technetium is similar, the same set of polypyridine ligands can be coordinated to $[Re(CO)_3]^+$ and $[^{99m}Tc(CO)_3]^+$ cores to yield luminescent probes and radioimaging reagents and -pharmaceuticals, respectively. Herein, we report the synthesis, characterization, and photophysical properties of a new class of luminescent rhenium(I) PEG-amine complexes $[Re(N^\wedge N)(CO)_3(py\text{-}PEG\text{-}NH_2)](PF_6)$ (py-PEG-NH_2 = 3-amino-5-(*N*-(2-(*ω*-methoxypoly(1-oxapropyl))-ethyl)aminocarbonyl)pyridine, MW_{PEG} = 5000 Da, PDI_{PEG} < 1.08; N^N = 1,10-phenanthroline (phen) (**1-PEG-NH$_2$**), 3,4,7,8-tetramethyl-1,10-phenanthroline (Me_4-phen) (**2-PEG-NH$_2$**), 4,7-diphenyl-1,10-phenanthroline (Ph_2-phen) (**3-PEG-NH$_2$**)), and $[Re(bpy\text{-}PEG)(CO)_3(py\text{-}NH_2)](PF_6)$ (bpy-PEG = 4-(*N*-(2-(*ω*-methoxypoly(1-oxapropyl))ethyl)-aminocarbonyl)-4′-methyl-2,2′-bipyridine; py-NH_2 = 3-aminopyridine) (**4-PEG-NH$_2$**) (Chart 1). The lipophilicity, water solubility, cytotoxic activity, and cellular uptake properties of these complexes have been compared to those of their PEG-free counterparts $[Re(N^\wedge N)(CO)_3(py\text{-}Et\text{-}NH_2)](PF_6)$ (py-Et-NH_2 = 3-amino-5-(*N*-(ethyl)aminocarbonyl)pyridine; N^N = phen (**1-Et-NH$_2$**), Me_4-phen (**2-Et-NH$_2$**), Ph_2-phen (**3-Et-NH$_2$**)) and $[Re(bpy\text{-}Et)(CO)_3(py\text{-}NH_2)](PF_6)$ (bpy-Et = 4-(*N*-(ethyl)aminocarbonyl)-4′-methyl-2,2′-bipyridine) (**4-Et-NH$_2$**) (Chart 1). The amine complexes **1-PEG-NH$_2$**−**4-PEG-NH$_2$** have been activated with thiophosgene to yield the isothiocyanate complexes $[Re(N^\wedge N)(CO)_3(py\text{-}PEG\text{-}NCS)](PF_6)$ (py-PEG-NCS = 3-isothiocyanato-5-(*N*-(2-(*ω*-methoxypoly(1-oxapropyl))ethyl)aminocarbonyl)pyridine; N^N = phen (**1-PEG-NCS**), Me_4-phen (**2-PEG-NCS**), Ph_2-phen (**3-PEG-NCS**)) and $[Re(bpy\text{-}PEG)(CO)_3(py\text{-}NCS)](PF_6)$ (py-NCS = 3-isothiocyanatopyridine) (**4-PEG-NCS**) (Chart 1) as a new class of luminescent PEGylation reagents. To examine their PEGylation properties, these isothiocyanate complexes have been reacted with a model substrate *n*-butylamine, resulting in the formation of the thiourea complexes $[Re(N^\wedge N)(CO)_3(py\text{-}PEG\text{-}Bu)](PF_6)$ (py-PEG-Bu = 3-*n*-butylthioureidyl-5-(*N*-(2-(*ω*-methoxypoly(1-oxapropyl))ethyl)aminocarbonyl)pyridine; N^N = phen (**1-PEG-Bu**), Me_4-phen (**2-PEG-Bu**), Ph_2-phen (**3-PEG-Bu**)) and $[Re(bpy\text{-}PEG)(CO)_3(py\text{-}Bu)](PF_6)$ (py-Bu = 3-*n*-butylthioureidylpyridine) (**4-PEG-Bu**) (Chart 1). Additionally, bovine serum albumin (BSA) and poly(ethyleneimine) (PEI) have been PEGylated with the isothiocyanate complexes to yield the luminescent bioconjugates **1-PEG-BSA**−**4-PEG-BSA** and **1-PEG-PEI**−**4-PEG-PEI**, respectively. The DNA-binding and polyplex-formation properties of conjugate **3-PEG-PEI** have been studied and compared with those of unmodified PEI. Furthermore, the in vivo toxicity of complex **3-PEG-NH$_2$** and its PEG-free counterpart **3-Et-NH$_2$** has been investigated using zebrafish embryos as an animal model.

RESULTS AND DISCUSSION

Design and Synthesis of Complexes. Regarding the design of the PEG complexes, different diimine ligands (phen, Me_4-phen, Ph_2-phen, and bpy-PEG) have been used to investigate the effects of the methyl, phenyl, and amide substituents on various physical and biological properties of the complexes. The PEG pendant was linked to the complexes via the use of the monodentate py-PEG-NH_2 and bidentate bpy-PEG ligands, which were synthesized from the reactions of 3-amino-5-carboxysuccinimidylpyridine (py-NHS-NH_2) and 4-carboxysuccinimidyl-4′-methyl-2,2′-bipyridine (bpy-NHS), respectively, with *α*-amino-*ω*-methoxypoly(ethylene glycol) ($mPEG_{5000}$-NH_2). Complexes **1-PEG-NH$_2$**−**4-PEG-NH$_2$** and their PEG-free counterparts **1-Et-NH$_2$**−**4-Et-NH$_2$** were obtained from the reaction of $[Re(N^\wedge N)(CO)_3(CH_3CN)](CF_3SO_3)$ with the respective pyridine ligands, followed by anion exchange with KPF_6 and purification. The isothiocyanate complexes **1-PEG-NCS**−**4-PEG-NCS** were obtained from the reaction of the amine complexes **1-PEG-NH$_2$**−**4-PEG-NH$_2$** with thiophosgene in acetone at room temperature. To examine the reactivity of the isothiocyanate complexes toward primary amines, they have been reacted with a model substrate, *n*-butylamine, yielding the thiourea complexes **1-PEG-Bu**−**4-PEG-Bu**. These complexes were purified by size exclusion chromatography and microfiltration. All the complexes have been characterized by ^{1}H NMR, IR spectroscopy, ESI-MS (or MALDI-TOF-MS for the PEG complexes), and elemental analysis (for the non-PEG complexes). The molecular weight difference of complexes **1-PEG-NH$_2$**−**3-PEG-NH$_2$** and the ligand py-PEG-NH_2, respectively, was found to be about 500 Da in the MALDI-TOF mass spectra (Supporting Information, Figure S1), which is in agreement with the mass of the corresponding $[Re(N^\wedge N)(CO)_3]$ unit.

Electronic Absorption and Emission Properties. The electronic absorption spectral data of all the complexes are summarized in Supporting Information, Table S1. All the complexes displayed intense absorption bands at about 250−345 nm with extinction coefficients on the order of 10^4 dm^3 mol^{-1} cm^{-1}, which have been assigned to spin-allowed intraligand (^{1}IL) ($\pi \rightarrow \pi^*$) (N^N and pyridine ligands) transitions.[16−26] The lower-energy absorption shoulders at about 366−396 nm, with extinction coefficients on the order of 10^3 dm^3 mol^{-1} cm^{-1}, have been assigned to spin-allowed metal-to-ligand charge-transfer (^{1}MLCT) ($d\pi(Re) \rightarrow \pi^*(N^\wedge N)$) transitions.

Upon photoexcitation, all the complexes displayed intense and long-lived green to orange emission. The photophysical data are summarized in Table 1, and the emission spectra of the PEG-amine complexes **1-PEG-NH$_2$**−**3-PEG-NH$_2$** in CH_3CN at 298 K are shown in Figure 1. In fluid solutions at 298 K, most of the complexes displayed reduced emission energy, quantum yields, and lifetimes upon increasing the polarity of the solvents. These findings, together with the dependence of the emission energy on the π^* orbital energy level of the N^N ligands, point to an emissive state of ^{3}MLCT ($d\pi(Re) \rightarrow \pi^*(N^\wedge N)$) character. The structural features and long emission lifetimes of the Me_4-phen complexes in fluid solutions under ambient conditions suggest the involvement of ^{3}IL ($\pi \rightarrow \pi^*$)

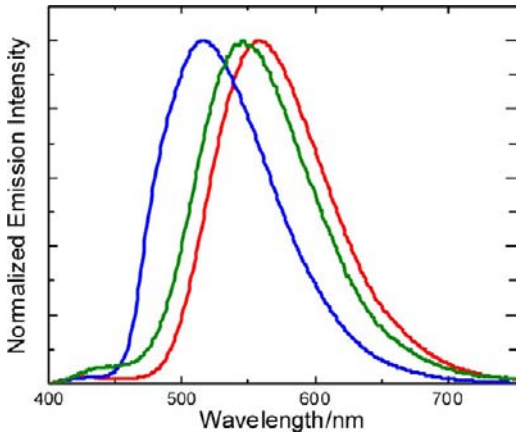

Figure 1. Emission spectra of complexes **1-PEG-NH$_2$** (green), **2-PEG-NH$_2$** (blue), and **3-PEG-NH$_2$** (red) in CH_3CN at 298 K.

(Me_4-phen) character in their emissive states. In low-temperature glass, the Me_4-phen complexes displayed even richer structural features in their emission spectra, as exemplified by that of complex **2-PEG-NH$_2$** (Supporting Information, Figure S2). Also, double-exponential decay was observed, with shorter- and longer-lived components of about 30 to 40 and 110 to 150 μs, respectively (Table 1), which have been attributed to ^{3}MLCT ($d\pi$(Re) $\rightarrow$ π^*(Me_4-phen)) and ^{3}IL ($\pi \rightarrow \pi^*$) (Me_4-phen) emissive states. Interestingly, while the PEG pendants did not significantly perturb the emission energy of the rhenium–amine complexes, the emission quantum yields of the PEG-amine complexes are lower than those of their PEG-free counterparts in CH_2Cl_2 and CH_3CN. It is conceivable that the long and flexible PEG pendant facilitates the nonradioactive decay of the PEG complexes, as reflected by the generally large k_{nr} values of these complexes compared to the PEG-free complexes (Table 1),[26e] which subsequently lead to lower emission quantum yields. Although complex **2-PEG-NH$_2$** displayed a lower emission quantum yield, unexpectedly, it exhibited a longer emission lifetime than its PEG-free counterpart **2-Et-NH$_2$**, which may be related to the ^{3}IL character of the emissive states. In aqueous buffer, all the PEG-amine complexes displayed smaller k_{nr} values and higher emission quantum yields than their PEG-free counterparts (Table 1). We have tentatively attributed this observation to the self-wrapping of the rhenium(I)-diimine core by the PEG chain, which is expected to shield the luminophore from interacting with the water molecules and buffer ions, resulting in less efficient nonradiative decay and an increased emission quantum yield. Similar findings have also been observed in related rhenium(I) polypyridine complexes modified with long aliphatic chains.[27] It is noteworthy that the isothiocyanate complexes **1-PEG-NCS–4-PEG-NCS** emitted at higher energy than their amine **1-PEG-NH$_2$–4-PEG-NH$_2$** and thiourea **1-PEG-Bu–4-PEG-Bu** counterparts. We have ascribed this to the strongly electron-withdrawing isothiocyanate group, which stabilizes the $d\pi$(Re) orbitals and hence causes higher ^{3}MLCT emission energy. Nonetheless, the energy difference is small because the electron density of the rhenium(I) center is only remotely influenced by the substituents on the pyridine ligand.

Lipophilicity and Water Solubility. The lipophilicity (log $P_{o/w}$) of the PEG-amine complexes **1-PEG-NH$_2$–4-PEG-NH$_2$** and their PEG-free counterparts **1-Et-NH$_2$–4-Et-NH$_2$** has been determined by the flask-shaking method, and the results are listed in Table 2. We found that the lipophilicity of the complexes depended on the diimine ligands and followed the order: Ph_2-phen > Me_4-phen ≈ bpy-amide > phen, which is in accordance with the hydrophobic character of the ligands. The PEG complexes **1-PEG-NH$_2$–4-PEG-NH$_2$** (log $P_{o/w}$ = −0.87 to −1.70) exhibited substantially lower lipophilicity than their PEG-free counterparts **1-Et-NH$_2$–4-Et-NH$_2$** (log $P_{o/w}$ = 0.81 to 2.04), reflecting the highly hydrophilic nature of the PEG pendants. Importantly, the water solubility of the PEG-NH$_2$ complexes (from 13.1 to 47.5 mM) is significantly higher than that of the PEG-free analogues (from 0.02 to 2.7 mM) (Table 2). The high water solubility of the PEG complexes is obviously an advantage that would render the complexes useful reagents for various biological applications.

Table 2. Lipophilicity (log $P_{o/w}$) and Water Solubility of Complexes 1-PEG-NH$_2$–4-PEG-NH$_2$ and 1-Et-NH$_2$–4-Et-NH$_2$

complex	log $P_{o/w}$	water solubility/mM
1-PEG-NH$_2$	−1.70 ± 0.04	47.5
2-PEG-NH$_2$	−0.94 ± 0.02	13.1
3-PEG-NH$_2$	−0.87 ± 0.05	39.7
4-PEG-NH$_2$	−1.04 ± 0.01	28.7
1-Et-NH$_2$	0.81 ± 0.03	0.36
2-Et-NH$_2$	1.09 ± 0.03	0.19
3-Et-NH$_2$	2.04 ± 0.05	0.016
4-Et-NH$_2$	1.37 ± 0.06	2.66

Cellular Uptake Properties and Live-Cell Confocal Imaging. The cellular uptake properties of the PEG-amine complexes **1-PEG-NH$_2$–4-PEG-NH$_2$** and their PEG-free counterparts **1-Et-NH$_2$–4-Et-NH$_2$** have been studied by ICP-MS. Upon incubation with the complexes at 37 °C for 3 h, an average HeLa cell (volume = 3.4 pL) contained 0.09 to 2.99 fmol of rhenium (Table 3), which is comparable to related rhenium(I) complexes in other studies such as [Re(phen)(CO)$_3$(py-TU-DPAT)](CF_3SO_3) (py-TU-DPAT = 3-(2-(4-hydroxy-3-(2,2′-dipicolylaminomethyl)phenyl)-ethylthioureidyl)pyridine) (2.8 fmol of rhenium)[24] and [Re(phen)(CO)$_3$(py-3-glu)](PF_6) (py-3-glu = 3-(*N*-(6-(*N*′-(4-(α-D-glucopyranosyl)phenyl)thioureidyl)hexyl)thioureidyl)-pyridine) (1.10 fmol of rhenium).[26i] The PEG-amine complexes displayed less effective cellular uptake than their PEG-free counterparts, which is probably due to their lower

Table 3. Numbers of Moles of Rhenium(I) Associated with an Average HeLa Cell upon Incubation with Complexes 1-PEG-NH$_2$–4-PEG-NH$_2$ and 1-Et-NH$_2$–4-Et-NH$_2$ at 37 °C for 3 h[a]

complex	no. of mol/fmol	concentration/mM
1-PEG-NH$_2$	0.21 ± 0.03	0.06 ± 0.008
2-PEG-NH$_2$	0.37 ± 0.02	0.11 ± 0.006
3-PEG-NH$_2$	0.40 ± 0.01	0.12 ± 0.003
4-PEG-NH$_2$	0.09 ± 0.01	0.03 ± 0.001
1-Et-NH$_2$	0.27 ± 0.03	0.08 ± 0.009
2-Et-NH$_2$	0.82 ± 0.02	0.24 ± 0.006
3-Et-NH$_2$	2.99 ± 0.07	0.88 ± 0.020
4-Et-NH$_2$	0.12 ± 0.03	0.04 ± 0.009

[a] [Re] = 10 μM in the incubation medium.

dx.doi.org/10.1021/ic301948d | *Inorg. Chem.* 2012, 51, 13289–13302

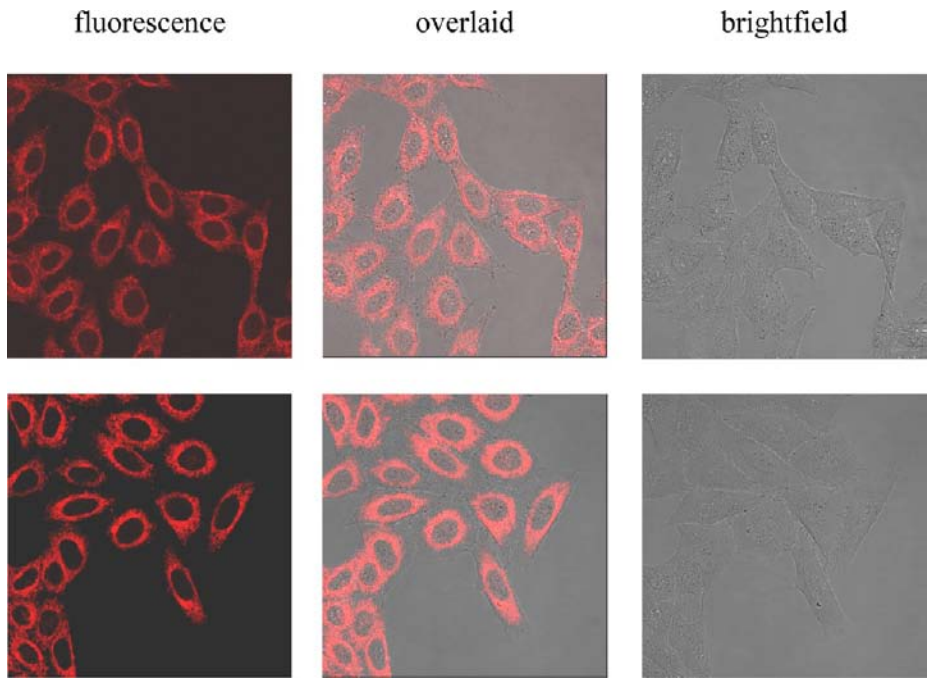

Figure 2. Laser-scanning confocal microscopy images of HeLa cells incubated with complexes **3-PEG-NH$_2$** (top row) and **3-Et-NH$_2$** (bottom row) (10 μM) at 37 °C for 1 h.

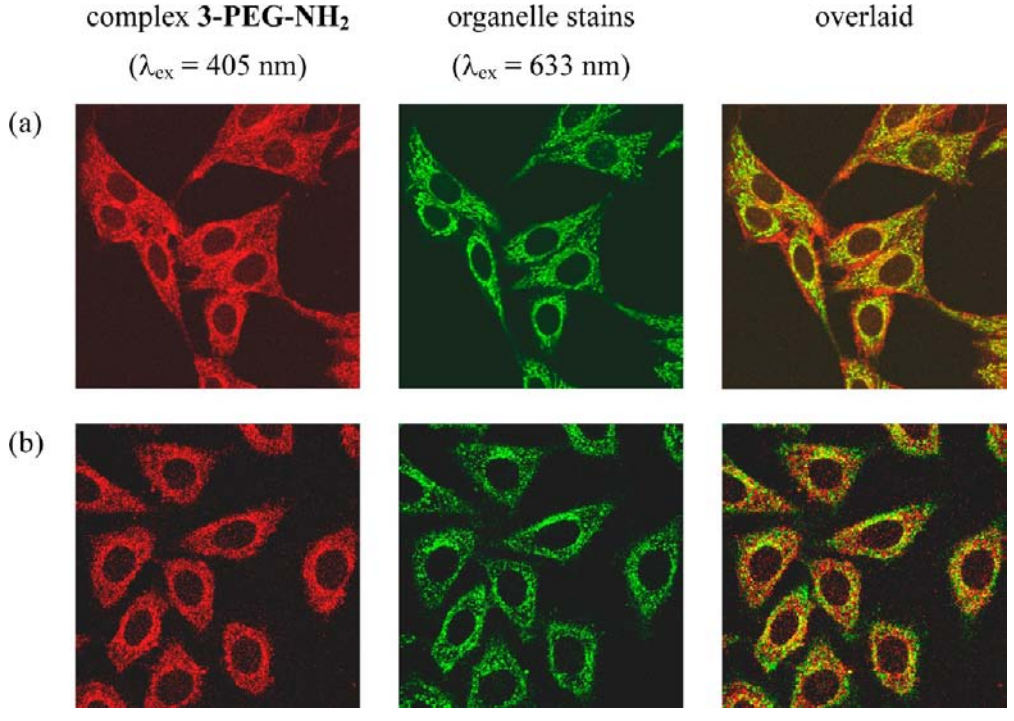

Figure 3. Laser-scanning confocal microscopy images of HeLa cells treated with complex **3-PEG-NH$_2$** and (a) MitoTracker Deep Red FM and (b) Alexa Fluor 633-conjugated transferrin at 37 °C, respectively.

lipophilicity and larger molecular size. It is important to point out that the intracellular rhenium concentrations of all the complexes (0.03 to 0.88 mM) were much higher than that in the medium before the uptake (10 μM), indicative of cellular accumulation of the complexes.

The biological properties of the Ph$_2$-phen complexes **3-PEG-NH$_2$** and **3-Et-NH$_2$** have been studied in more detail. The laser-scanning confocal microscopy images of HeLa cells treated with these complexes (10 μM, 1 h) showed that they were effectively internalized and localized in the cytoplasmic region (Figure 2). Thus, the PEG pendant of complex **3-PEG-NH$_2$** did not significantly affect its intracellular localization properties. Also, the nuclei showed much weaker or no emission, indicative of negligible nuclear uptake. HeLa cells incubated with complex **3-PEG-NH$_2$** emitted weaker than those loaded with complex **3-Et-NH$_2$**, which is a result of the lower uptake efficiency of the former complex. To examine the intracellular localization properties of the PEG complexes,

dx.doi.org/10.1021/ic301948d | *Inorg. Chem.* 2012, 51, 13289−13302

HeLa cells have been co-stained with complex **3-PEG-NH$_2$** and MitoTracker Deep Red FM (a mitochondrial marker) and Alexa Fluor 633-conjugated transferrin (an endosomal marker), respectively. The images showed that the complex was co-localized with the mitochondrial and endosomal markers with co-localization coefficients of 71.6% and 18.2%, respectively, suggesting that the PEG complex **3-PEG-NH$_2$** is enriched in the mitochondria (Figure 3). Similar mitochondria-targeting behavior has been observed in other rhenium(I) polypyridine complexes.[26j]

Cytotoxicity. The cytotoxicity of the PEG-amine complexes **1-PEG-NH$_2$**−**4-PEG-NH$_2$** and their PEG-free counterparts **1-Et-NH$_2$**−**4-Et-NH$_2$** toward HeLa cells over an incubation period of 48 h have been investigated by the MTT assay (Table 4). In both series of complexes, the Ph$_2$-phen and Me$_4$-phen

Table 4. Cytotoxicity (IC_{50}, 48 h) of Complexes 1-PEG-NH$_2$−4-PEG-NH$_2$ and 1-Et-NH$_2$−4-Et-NH$_2$ and Cisplatin toward HeLa Cells

complex	$IC_{50}/\mu M$
1-PEG-NH$_2$	26.3 ± 1.6
2-PEG-NH$_2$	11.9 ± 1.6
3-PEG-NH$_2$	6.6 ± 0.4
4-PEG-NH$_2$	>1151.7
1-Et-NH$_2$	15.0 ± 4.8
2-Et-NH$_2$	5.0 ± 0.4
3-Et-NH$_2$	3.6 ± 0.4
4-Et-NH$_2$	159.1 ± 8.0
cisplatin	11.9 ± 0.3

complexes showed higher cytotoxicity, which has been ascribed to their higher lipophilicity and uptake efficiency. Similar observations have been reported in related studies.[26i,j] We also noted that the PEG complexes were less cytotoxic than their PEG-free counterparts, which has been attributed to the long and flexible PEG pendants which prevent the complexes from interacting nonspecifically with extracellular proteins and triggering immunogenicity and antigenicity inside the cells.[28] Remarkably, the bpy-PEG complex **4-PEG-NH$_2$** displayed extraordinarily low cytotoxicity, with an IC_{50} value of >1152 μM, which is at least 7 times lower than that of its PEG-free counterpart **4-Et-NH$_2$** (IC_{50} = 159.1 μM). Apparently, the low lipophilicity and uptake efficiency of this complex alone cannot account for this result. One possible reason is that the PEG pendant of this complex is linked to the diimine ligand, which may provide more effective wrapping of the complex, resulting in much enhanced biocompatibility.

PEGylation of BSA and PEI. To evaluate their PEGylation properties, the isothiocyanate complexes **1-PEG-NCS**−**4-PEG-NCS** have been used to label a model protein, BSA, via the reaction of the isothiocyanate group with the primary amines of the lysine residues. The resultant bioconjugates **1-PEG-BSA**−**4-PEG-BSA** were purified by size exclusion chromatography and ultrafiltration. The electronic absorption spectra of the bioconjugates have been measured and that of bioconjugate **1-PEG-BSA** is shown in Figure 4 as an example. The spectra displayed an intense absorption band at 280 nm, which is attributed to both the protein and the complexes, and a shoulder at about 328−371 nm, which is solely due to the rhenium(I) complexes. On the basis of the spectroscopic data, the rhenium-to-protein ratios of bioconjugates **1-PEG-BSA**−**4-PEG-BSA** have been determined to be about 2.2, 2.7, 2.9, and

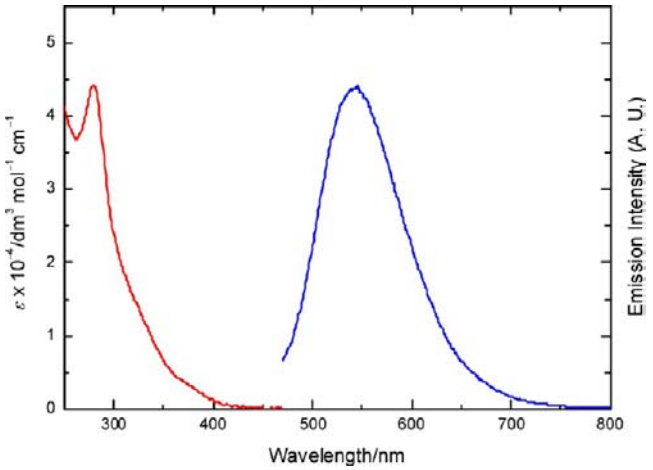

Figure 4. Electronic absorption (red) and emission (blue) spectra of bioconjugate **1-PEG-BSA** in degassed 50 mM potassium phosphate buffer at pH 7.4 at 298 K.

3.8, respectively. Upon photoexcitation, all the bioconjugates showed intense and long-lived green to orange-yellow ^{3}MLCT/^{3}IL emission in 50 mM potassium phosphate buffer pH 7.4 at 298 K (Table 5). The emission spectrum of

Table 5. Photophysical Data of Bioconjugates 1-PEG-BSA−4-PEG-BSA and 1-PEG-PEI−4-PEG-PEI in Degassed 50 mM Potassium Phosphate Buffer at pH 7.4 at 298 K

bioconjugate	λ_{em}/nm	$\tau_o/\mu s$	Φ_{em}
1-PEG-BSA	541	0.58 (39%), 1.29 (61%)	0.018
2-PEG-BSA	485 sh, 516	3.26 (23%), 10.78 (77%)	0.041
3-PEG-BSA	562	1.66 (26%), 4.70 (74%)	0.013
4-PEG-BSA	566	0.10 (18%), 0.41 (82%)	0.0071
1-PEG-PEI	552	0.96	0.014
2-PEG-PEI	484 sh, 520	3.89	0.012
3-PEG-PEI	565	1.86	0.0045
4-PEG-PEI	584	0.08	0.0022

bioconjugate **1-PEG-BSA** is shown in Figure 4. While the emission wavelengths of bioconjugates **1-PEG-BSA**−**3-PEG-BSA** were similar to those of their thiourea counterparts **1-PEG-Bu**−**3-PEG-Bu**, respectively, bioconjugate **4-PEG-BSA** emitted at higher energy than **4-PEG-Bu** (Table 1). This observation may originate from the hydrophobic nature of the protein surface since the emission of common [Re(N^N)-(CO)$_3$(py)]$^+$ complexes occurs at higher energy in more nonpolar solvents, with higher environment-sensitivity of the bpy-amide ligand compared to the other diimine ligands (phen, Me$_4$-phen, and Ph$_2$-phen).[26e,g] Another interesting observation is that all the bioconjugates displayed biexponential decay (Table 5), which is common for biomolecules labeled with luminescent transition metal complexes.[25a,b,29] It is noteworthy that the average emission lifetimes of bioconjugates **1-PEG-BSA**−**4-PEG-BSA** (from 0.39 to 10.16 μs) are longer than those of the thiourea complexes **1-PEG-Bu**−**4-PEG-Bu** (from 0.08 to 4.21 μs) as a result of the more hydrophobic and rigid local environment associated with the protein molecules.

The use of polyamines in gene delivery and cancer therapy has attracted much attention. In this context, PEI has been commonly used as a DNA condensing and gene delivery reagent because of its high positive charge density and high proton buffer capacity over a wide pH range.[30] Since PEI does

dx.doi.org/10.1021/ic301948d | Inorg. Chem. 2012, 51, 13289−13302

not absorb or emit in the UV−vis region, it has been modified with various reporters so that its cellular uptake and gene delivery properties can be readily investigated by fluorescence methods; for example, PEI has been conjugated with fluorescent organic dyes and phosphorescent transition metal complexes to study the cellular uptake and intracellular transport pathways of PEI/DNA polyplexes.[15,31] Also, since PEI is cytotoxic to many cell types, it is commonly PEGylated to lower its cytotoxicity, to increase the water solubility of the PEI/DNA polyplexes, and to facilitate transfection applications.[32] In this work, we have PEGylated PEI (25 kDa) with the isothiocyanate complexes **1-PEG-NCS−4-PEG-NCS** to generate a new class of luminescent vectors for transfection studies. The resultant conjugates **1-PEG-PEI−4-PEG-PEI** were purified by size exclusion chromatography and ultrafiltration. On the basis of the spectroscopic data, the rhenium-to-PEI ratios of conjugates **1-PEG-PEI−4-PEG-PEI** have been determined to be about 21.6, 13.6, 8.4, and 13.7, respectively. These are larger than those of the BSA conjugates **1-PEG-BSA−4-PEG-BSA** (vide supra), most likely because of the higher number of primary amines available on the PEI polymer. Upon photoexcitation, all the PEI conjugates displayed long-lived green to orange-yellow ^{3}MLCT/^{3}IL emission in 50 mM potassium phosphate buffer pH 7.4 at 298 K. The emission maxima of these PEI conjugates (520−584 nm) occurred at slightly lower energy than their BSA counterparts (Table 5). These results illustrate the highly polar nature of the protonated amine groups of the PEI moiety in an aqueous environment. Interestingly, these findings are also in accordance with the shorter emission lifetimes and lower quantum yields of the PEI conjugates compared to both the corresponding BSA conjugates (Table 5) and the thiourea complexes **1-PEG-Bu−4-PEG-Bu** (Table 1). Thus, in aqueous buffer, the rhenium(I) polypyridine PEG complexes experience the most hydrophobic environment on BSA molecule, whereas the polycationic nature of the PEI polymer would offer the most hydrophilic surroundings. This also highlights the environment-sensitive emission properties of this class of complexes, which render them useful reporters of their local environments.

DNA-Binding and Transfection Properties. We have investigated the DNA-binding properties of conjugate **3-PEG-PEI** by agarose gel electrophoresis. Polyplexes formed from this conjugate and the pDNA pRL-TK with N/P ratios from 1 to 32 have been prepared prior to the analysis. Polyplexes prepared with unmodified PEI and pRL-TK were used as a control. As shown in Figure 5, conjugate **3-PEG-PEI** retarded the pDNA with increasing N/P ratios, revealing that the positively charged PEI conjugate neutralizes the negative charge of the pDNA. The migration of DNA bands of polyplexes **3-PEG-PEI**/pRL-TK and PEI/pRL-TK was completely retarded at N/P ratios = 8 and 4, respectively (Figure 5). This result illustrates that the DNA condensation ability of PEI was reduced upon conjugation with the PEG complex.

The zeta potentials and mean hydrodynamic diameters of the polyplexes **3-PEG-PEI**/pRL-TK and unmodified PEI/pRL-TK have been studied by dynamic light scattering. The polyplexes **3-PEG-PEI**/pRL-TK displayed negative zeta potentials from −31.8 to −1.0 mV with N/P ratios from 1 to 8, and acquired a significant increase of zeta potentials to +1.1 and +5.8 mV at N/P ratios = 16 and 32, respectively (Table 6). The trend observed for the unmodified PEI/pRL-TK is similar, except that a positive zeta potential (+3.4 mV) appears when the N/P ratio arrives at 8. This is in agreement with the gel electrophoresis results since the polyplexes at N/P ratios ≥8 or 4 were retarded in the agarose gel for **3-PEG-PEI**/pRL-TK and unmodified PEI/pRL-TK, respectively (Figure 5). The hydrodynamic diameters of the polyplexes **3-PEG-PEI**/pRL-TK increased from about 260 to 390 nm upon increasing the N/P ratio from 1 to 8, and decreased at higher N/P ratios (16 and 32). Similarly, the size of unmodified PEI/pRL-TK increased from 226 to 816 nm (with N/P ratios from 1 to 4) and subsequently decreased to 249 nm at N/P ratio = 32. These observations support the argument that the positively charged PEI conjugate condensed the negative pDNA efficiently and formed more compact polyplexes at N/P ratios ≥8 and 4, respectively for the two series of polyplexes. Similar expansion and shrinking of hydrodynamic diameters are commonly observed in other amphiphile/DNA polyplexes.[33] Interestingly, the increase is less prominent for the polyplexes **3-PEG-PEI**/pRL-TK than the unmodified PEI/pRL-TK, which is attributable to the fact that aggregation of the polyplexes can be prevented by PEG pendants.

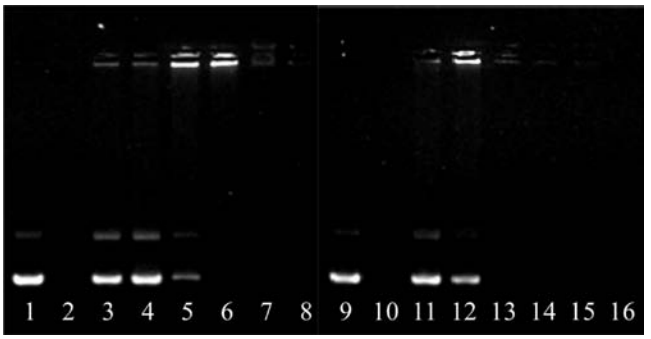

Figure 5. Gel electrophoresis of polyplexes **3-PEG-PEI**/pRL-TK and PEI/pRL-TK with different N/P ratios. Lane 1: DNA only; Lane 2: conjugate **3-PEG-PEI** only; Lane 3 to 8: polyplexes **3-PEG-PEI**/pRL-TK with N/P ratios = 1, 2, 4, 8, 16, and 32, respectively; Lane 9: DNA only; Lane 10: PEI only; Lane 11 to 16: polyplexes PEI/pRL-TK with N/P ratios = 1, 2, 4, 8, 16, and 32, respectively.

The in vitro transfection efficiency of conjugate **3-PEG-PEI** has been examined using HeLa cells and the plasmid pRL-TK that expresses luciferase via formation of polyplexes with N/P ratios from 1 to 32. Lipofactamine/pRL-TK and naked pDNA were used as a positive and negative control, respectively, and the results are shown in Figure 6. The transfection efficiency of polyplexes **3-PEG-PEI**/pRL-TK and unmodified PEI/pRL-TK was the highest at N/P ratios = 16 and 8, respectively, which is generally in line with the gel electrophoresis results (Figure 5). Although the transfection efficiency of conjugate **3-PEG-PEI** was weaker than PEI at N/P ratio = 8, its transfection ability was higher at higher N/P ratios, that is, 16 and 32. Actually, at N/P = 32, the transfection ability of unmodified PEI was much lower. All these observations can be ascribed to the lower cytotoxicity of conjugate **3-PEG-PEI** due to the PEG units. Additionally, the intracellular localization of the polyplex **3-PEG-PEI**/pRL-TK (4 μg pDNA; N/P = 16) has been investigated by laser-scanning confocal microscopy. HeLa cells treated with the polyplex showed punctate cytoplasmic staining with negligible nuclear uptake (Figure 7). All these results demonstrated that the transfection properties of PEI are retained after PEGylation by complex **3-PEG-NCS** and the intracellular localization properties of the PEGylated PEI

Table 6. Zeta Potentials and Mean Hydrodynamic Diameters of Polyplexes 3-PEG-PEI/pRL-TK and PEI/pRL-TK with Different N/P Ratios in Tris-Cl Buffer (50 mM, pH = 7.4)

	zeta potential/mV		mean hydrodynamic diameter/nm	
N/P ratio	**3-PEG-PEI**/pRL-TK	PEI/pRL-TK	**3-PEG-PEI**/pRL-TK	PEI/pRL-TK
1	−31.8 ± 1.8	−33.3 ± 8.5	259.9 ± 5.3	225.5 ± 12.8
2	−30.1 ± 0.2	−25.5 ± 1.7	265.2 ± 42.9	234.2 ± 3.6
4	−24.5 ± 0.4	−7.8 ± 2.0	352.9 ± 10.7	815.5 ± 148.6
8	−1.0 ± 0.2	+3.4 ± 2.1	389.8 ± 20.3	713.0 ± 64.3
16	+1.1 ± 0.2	+28.3 ± 1.7	291.0 ± 43.8	234.9 ± 16.4
32	+5.8 ± 0.4	+37.9 ± 2.3	207.1 ± 25.9	248.5 ± 20.9

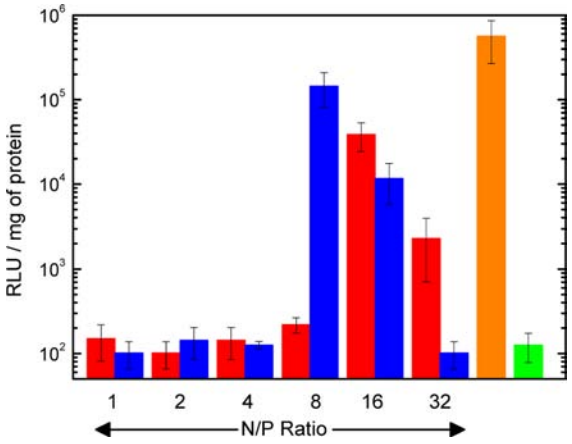

Figure 6. Luciferase activity (RLU/mg of protein) of HeLa cells incubated with polyplexes **3-PEG-PEI**/pRL-TK (red) and unmodified PEI/pRL-TK (blue) with different N/P ratios. Lipofectamine/pRL-TK (orange) and naked DNA (green) were used as a positive and negative control, respectively.

conjugate can be readily studied by optical spectroscopy and microscopy.

In Vivo Toxicity. We have selected zebrafish embryos as an animal model to examine the effects of the PEG pendants on the in vivo toxicity of the complexes. Selected 4 hours post fertilization (hpf) embryos were exposed to the PEG complex **3-PEG-NH$_2$** and its PEG-free counterpart **3-Et-NH$_2$**, respectively, and the LD_{50} values have been determined at five incubation time points (24, 48, 72, 96, and 120 hpf). The LD50 values for both complexes did not vary much in first 4 time points (24 to 96 hpf) (Table 7). As expected, the PEG complex exhibited higher LD_{50} values than its PEG-free counterpart at all time points studied, indicating that modification of the complex with a PEG unit reduces its in vivo toxicity. We have studied the hatching rates of the embryos incubated with complexes **3-PEG-NH$_2$** and **3-Et-NH$_2$**, and the results are shown in Figure 8. The hatching percent was calculated from the total number of hatched larvae relative to the total number of surviving embryos and larvae at each concentration. In the control experiments without any rhenium(I) complexes added, about 60% of the embryos hatched in 72 hpf and over 95% of them in 96 hpf. It is noteworthy that the embryos incubated with the complexes at lower concentrations (from 0.31 to 5 μM) showed a similar hatching rate to the controls. However, at higher complex concentrations (10 and 20 μM), while none of the embryos incubated with complex **3-Et-NH$_2$** hatched successfully, most of those incubated with the PEG complex **3-PEG-NH$_2$** hatched but with a delayed hatching time. The hatching percentage of the embryos at [**3-PEG-NH$_2$**] = 10 μM was only about 20% in 72 hpf and 80% in 120 hpf. At [**3-PEG-NH$_2$**] = 20 μM, the hatching of the embryos was suppressed significantly, and less than 60% of the embryos hatched in 120 hpf. It is likely that the delayed hatching is due to hypoxia because the PEG complex was found to adhere to the external surface of the chorion upon incubation, as revealed by the fluorescence and brightfield microscopy images in Figure 9 (top row), which is likely to interfere with oxygen and nutrients exchange. Related studies have also shown that hypoxia significantly affects embryonic development; for example, sand snail (*Polinices sordidus*) displays delayed hatching under hypoxic conditions.[34] Similar hatching delay has also been observed for the zebrafish embryos incubated with single-wall carbon nanotubes.[35] It is important to point out that although the PEG complex caused delayed hatching, all the successfully hatched larvae did not show any defects. These results further support that modification of the rhenium complex with a PEG unit is an efficient method to lower its in vivo toxicity and enhance its biocompatibility.

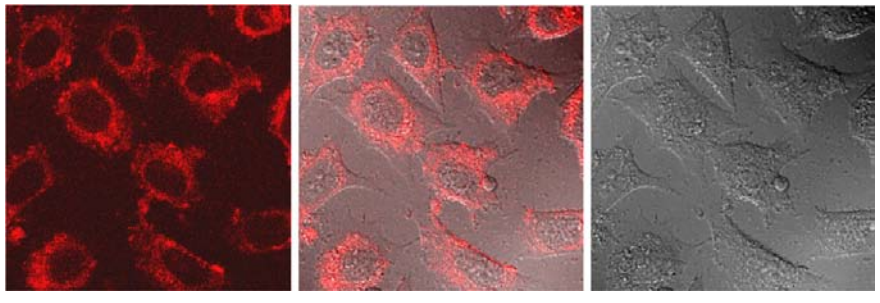

Figure 7. Fluorescence (left), overlaid (middle), and brightfield (right) microscopy images of HeLa cells incubated with the polyplex **3-PEG-PEI**/pRL-TK (4 μg pDNA, N/P = 16) at 37 °C for 5 h.

dx.doi.org/10.1021/ic301948d | *Inorg. Chem.* 2012, 51, 13289−13302

Table 7. In Vivo Toxicity of Complexes 3-PEG-NH_2 and 3-Et-NH_2 toward Zebrafish Embryos at Different Incubation Time Points

	LD_{50} at different incubation time points/μM				
complex	24 hpf	48 hpf	72 hpf	96 hpf	120 hpf
3-PEG-NH_2	>40	>40	>40	>40	20.7 ± 3.0
3-Et-NH_2	5.4 ± 0.3	5.4 ± 0.3	5.4 ± 0.3	5.4 ± 0.3	5.3 ± 0.2

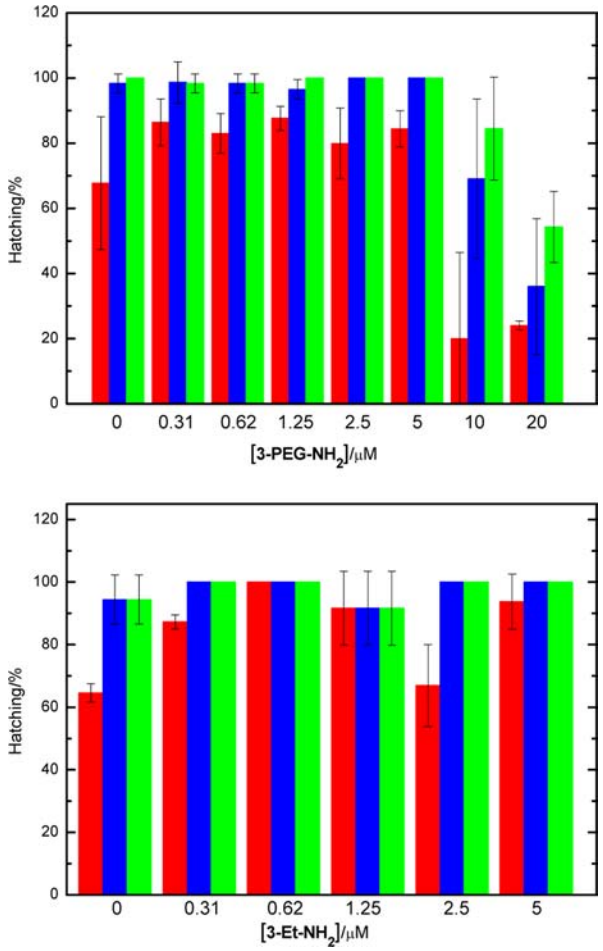

Figure 8. Hatching efficiency of zebrafish embryos after exposure to complexes **3-PEG-NH_2** (top) and **3-Et-NH_2** (bottom), respectively, at 72 (red), 96 (blue), and 120 (green) hpf at 28.5 °C.

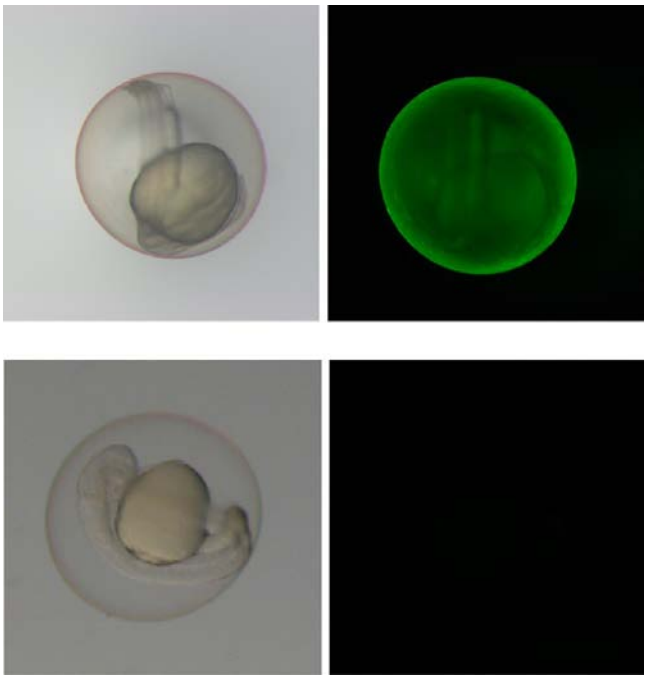

Figure 9. Brightfield (left) and fluorescence (right) microscopy images of 24-hpf zebrafish embryos incubated with complex **3-PEG-NH_2** (20 μM) at 28.5 °C for 20 h (top row). Bottom row: a control experiment in which the embryo was not treated with the complex.

CONCLUSION

In this work, a series of luminescent rhenium(I) polypyridine PEG-amine complexes **1-PEG-NH_2**−**4-PEG-NH_2** has been synthesized and characterized. Upon photoexcitation, these complexes displayed intense and long-lived ^{3}MLCT/^{3}IL emission. The PEG complexes exhibited increased water solubility and biocompatibility compared to their PEG-free counterparts **1-Et-NH_2**−**4-Et-NH_2**. The amine group of complexes **1-PEG-NH_2**−**4-PEG-NH_2** was activated by thiophosgene to yield the amine-specific PEGylation reagents **1-PEG-NCS**−**4-PEG-NCS**, which have been used to label *n*-butylamine, BSA, and PEI, respectively. All the resultant conjugates have been isolated, purified, and their photophysical properties have been investigated. The DNA-binding properties of the PEI conjugate **3-PEG-PEI** have been studied, and polyplexes formed from this conjugate and pDNA with different N/P ratios have also been characterized. Furthermore, the transfection properties of conjugate **3-PEG-PEI** have been investigated by luciferase assays, and the results showed that the transfection properties of PEI are retained after PEGylation by complex **3-PEG-NCS**. Thus, conjugate **3-PEG-PEI** serves as a novel phosphorescent transfection reagent for eukaryotic cells, which are expected to offer new insights in understanding the cellular uptake, intracellular trafficking, and DNA-delivery properties of PEI molecules.

Compared with their iridium(III) counterparts,[15] the effect of the appended PEG unit on the biocompatibility of the luminescent rhenium(I) PEG complexes in this work is less significant; for example, modification of the monodentate pyridine ligand with a PEG chain did not substantially lower the cytotoxicity of the rhenium(I) complexes, which we believe is due to the less effective coverage of the complex by the PEG. Unlike the iridium(III) system, where the attached PEG pendant alters the emissive state nature of the complexes, the rhenium(I) PEG complexes in this work emit at very similar energy to their PEG-free counterparts. However, both classes of complexes reveal increased emission quantum yields in aqueous buffer solutions, which is a consequence of the protection of excited complexes through wrapping by the PEG units. It is also obvious that the attachment of PEG to these transition metal complexes has substantially increased their water solubility, which is an important requirement for the design of biological probes. Related work on phosphorescent inorganic and

dx.doi.org/10.1021/ic301948d | *Inorg. Chem.* 2012, 51, 13289−13302

organometallic transition metal PEG and PEI complexes is in progress.

EXPERIMENTAL SECTION

Materials and Synthesis. All solvents were of analytical reagent grade and purified according to standard procedures.[36] Diimine ligands including phen, Ph_2-phen, and Me_4-phen, $AgCF_3SO_3$, 3-aminopyridine, KPF_6, $CaCO_3$, ethylamine, triethylamine, thiophosgene, and cisplatin were purchased from Acros. $Re(CO)_5Cl$ and branched PEI (MW = 25 kDa) were obtained from Aldrich. MTT, tricaine, and *n*-butylamine were purchased from Sigma. *α*-Amino-*ω*-methoxypoly(ethylene glycol) ($mPEG_{5000}$-NH_2) (MW_{PEG} = 5000 Da, PDI_{PEG} < 1.08) was purchased from Nanocs. All these chemicals were used without further purification. Py-NHS-NH_2,[37] bpy-NHS,[38] $[Re(N^N)(CO)_3(CH_3CN)](CF_3SO_3)$,[39] and bpy-Et[40] were prepared as described previously. BSA was obtained from Calbiochem. PD-10 size-exclusion columns and YM-30 centricons were purchased from GE Healthcare and Millipore, respectively. All buffer components were of biological grade and used as received. Autoclaved Milli-Q water was used for preparation of aqueous solutions. HeLa cells were obtained from American Type Culture Collection. Mature zebrafish were purchased from Chong Hing Aquarium, Hong Kong, China, and maintained as described by Westerfield.[41] The zebrafish embryos were obtained by photoinduced spawning over green plants and then cultured at 28.5 °C in filtered tap water with Instant Ocean (60 ng/mL), which was purchased from Aquatic System. MitoTracker Deep Red FM, Alexa Fluor 633-conjugated transferrin, UltraPure agarose, Dulbecco's modified Eagle's medium (DMEM), reduced serum medium (Opti-MEM), fetal bovine serum (FBS), phosphate buffered saline (PBS), Lipofectamine 2000, trypsin-EDTA, and penicillin/streptomycin were purchased from Invitrogen. Tris(hydroxymethyl)-aminomethane (Tris) from USB was used to prepare Tris-Cl (50 mM, pH 7.4). The plasmid DNA (pDNA) pRL-TK (4.0 kb) was amplified in *Escherichia coli* and purified by HiPure Filter Plasmid Kit, and the concentration of the pDNA was measured spectrophotometrically. The Renilla Luciferase Assay System was obtained from Promega and stored at −70 °C before use. The growth medium for cell culture contained DMEM with 10% FBS and 1% penicillin/streptomycin.

Py-PEG-NH_2. Py-NHS-NH_2 (114 mg, 0.48 mmol) was dissolved in hot DMF (20 mL) under an inert atmosphere of nitrogen. After the solution was cooled to room temperature, both $mPEG_{5000}$-NH_2 (800 mg, 0.16 mmol) (MALDI-TOF-MS: number average molecular weight (M_n) = 5253.95 Da, weight average molecular weight (M_w) = 5315.32 Da, PDI = 1.012) and triethylamine (0.1 mL) were added. The mixture was stirred under an inert atmosphere of nitrogen at room temperature for 48 h. The mixture was evaporated to dryness yielding a pale yellow solid which was redissolved in deionized water (10 mL). The solution was loaded onto a PD-10 size-exclusion column that had been equilibrated with water, and the solution containing the ligand was collected and lyophilized to give the product as a white solid. Yield: 744 mg (91%). ^{1}H NMR (300 MHz, $CDCl_3$, 298 K) δ 8.26 (d, 1 H, J = 1.5 Hz, H6 of pyridine), 8.05 (d, 1 H, J = 2.7 Hz, H2 of pyridine), 7.40 (t, 1 H, J = 2.1 Hz, H4 of pyridine), 7.21 (s, 1 H, py-3-CONH), 3.78−3.30 (m, ca. 452 H, $CONHCH_2$ and OCH_2 of PEG), 3.27 (s, 3 H, OCH_3). MALDI-TOF-MS: M_n = 5358.37 Da, M_w = 5372.21 Da, PDI = 1.003.

Py-Et-NH_2. Py-NHS-NH_2 (300 mg, 1.28 mmol) was dissolved in hot DMF (20 mL) under an inert atmosphere of nitrogen. After the solution was cooled to room temperature, both ethylamine in THF (2 M, 1.92 mL, 3.84 mmol) and triethylamine (0.1 mL) were added. The mixture was stirred under an inert atmosphere of nitrogen at room temperature for 24 h. The solution was evaporated to dryness yielding a pale yellow solid, which was purified by column chromatography on silica gel. The desired product was eluted with CH_2Cl_2/MeOH (30:1, v/v). The solvent was removed under vacuum to give the product as a white solid. Yield: 154 mg (73%). ^{1}H NMR (300 MHz, $CDCl_3$, 298 K) δ 8.28 (d, 1 H, J = 1.5 Hz, H6 of pyridine), 8.16 (d, 1 H, J = 2.4 Hz, H2 of pyridine), 7.43 (t, 1 H, J = 2.1 Hz, H4 of pyridine), 6.17 (s, 1 H, py-3-CONH), 3.50 (q, 2 H, J = 7.2 Hz, $NHCH_2CH_3$), 1.26 (t, 3 H, J = 7.5 Hz, $NHCH_2CH_3$). Positive-ion ESI-MS ion cluster at m/z 166 $\{M + H^+\}^+$.

Bpy-PEG. Bpy-NHS (94 mg, 0.40 mmol) was dissolved in hot DMF (20 mL) under an inert atmosphere of nitrogen. After the solution was cooled to room temperature, both $mPEG_{5000}$-NH_2 (500 mg, 0.10 mmol) (MALDI-TOF-MS: M_n = 5254.95 Da, M_w = 5315.32 Da, PDI = 1.012) and triethylamine (0.1 mL) were added. The mixture was stirred under an inert atmosphere of nitrogen at room temperature for 48 h. The mixture was evaporated to dryness yielding a pale yellow solid, which was redissolved in deionized water (10 mL). Any undissolved solid (excess bpy-NHS) was removed by centrifugation. The supernatant was loaded onto a PD-10 size-exclusion column that had been equilibrated with water, and the solution containing the ligand was collected and lyophilized to give the product as a white solid. Yield: 416 mg (81%). ^{1}H NMR (300 MHz, $CDCl_3$, 298 K) δ 8.77 (d, 1 H, J = 4.8 Hz, H6 of bpy), 8.67 (s, 1 H, H3 of bpy), 8.52 (d, 1 H, J = 5.4 Hz, H6′ of bpy), 8.23 (s, 1 H, H3′ of bpy), 7.77 (d, 1 H, J = 5.7 Hz, H5 of bpy), 7.44 (s, 1 H, bpy-CONH), 7.16 (d, 1 H, J = 5.1 Hz, H5′ of bpy), 3.87−3.38 (m, ca. 452 H, $CONHCH_2$ and OCH_2 of PEG), 3.35 (s, 3 H, OCH_3), 2.65 (s, 3 H, CH_3 of bpy). MALDI-TOF-MS: M_n = 5407.26 Da, M_w = 5420.97 Da, PDI = 1.003.

*Rhenium(I) Polypyridine Amine Complexes **1-PEG-NH_2**−**4-PEG-NH_2** and **1-Et-NH_2**−**4-Et-NH_2**.* A mixture of $[Re(N^N)(CO)_3(CH_3CN)](CF_3SO_3)$ (0.039 mmol) and the pyridine ligand py-PEG-NH_2 or py-Et-NH_2 (0.039 mmol) in THF (30 mL) was refluxed under an inert atmosphere of nitrogen for 12 h. The mixture was then evaporated to dryness. The complex was dissolved in MeOH, converted to the hexafluorophosphate salt by anion exchange with KPF_6, and then purified by column chromatography on alumina. The desired product was eluted with a mixture of CH_2Cl_2 and methanol, and it was subsequently recrystallized from a mixture of CH_2Cl_2 and diethyl ether.

*Rhenium(I) Polypyridine Isothiocyanate Complexes **1-PEG-NCS**−**4-PEG-NCS**.* Thiophosgene (15.6 μL, 0.20 mmol) was added to a mixture of the PEG-amine complex (0.020 mmol) and finely crushed $CaCO_3$ (26 mg, 0.20 mmol) in acetone (10 mL) under an inert atmosphere of nitrogen. The suspension was stirred in the dark at room temperature for 4 h. The mixture was filtered, and the filtrate was evaporated to dryness to give the product as a yellow solid.

*Rhenium(I) Polypyridine Thiourea Complexes **1-PEG-Bu**−**4-PEG-Bu**.* A mixture of the PEG isothiocyanate complex (0.01 mmol) and *n*-butylamine (0.04 mmol) in acetone (30 mL) was stirred under an inert atmosphere of nitrogen for 12 h. The mixture was evaporated to dryness to give a yellow solid, which was redissolved in deionized water (5 mL). Any undissolved solid was removed by centrifugation. The supernatant was loaded onto a PD-10 size-exclusion column that had been equilibrated with water, and the solution containing the complex was collected and lyophilized. Recrystallization of the crude product from CH_2Cl_2/diethyl ether afforded the complex as pale yellow crystals.

The characterization data of all the complexes are included in the Supporting Information.

Instrumentation and Methods. ^{1}H NMR spectra were recorded on a Varian Mercury 300 MHz NMR spectrometer at 298 K. Positive-ion ESI mass spectra were recorded on a Perkin-Elmer Sciex API 365 mass spectrometer. MALDI-TOF mass spectra were recorded on an Applied Biosystems 4800 plus MALDI-TOF/TOF analyzer. IR spectra were recorded on a Perkin-Elmer 1600 series FT-IR spectrophotometer. Elemental analyses were carried out on a Vario EL III CHN elemental analyzer. Electronic absorption and steady-state emission spectra were recorded on a Hewlett-Packard 8453 diode array spectrophotometer and a SPEX FluoroLog 3-TCSPC spectrophotometer equipped with a Hamamatsu R928 PMT detector, respectively. Emission lifetimes were measured in the Fast MCS or the MCS lifetime mode with a NanoLED N-375 as the excitation source. All the solutions for photophysical studies were degassed with at least four successive freeze−pump−thaw cycles and stored in a 10-cm^3 round-bottomed flask equipped with a side arm 1-cm fluorescence cuvette and sealed from the atmosphere by a Rotaflo HP6/6 quick-release Teflon stopper. Luminescence quantum yields were measured

dx.doi.org/10.1021/ic301948d | *Inorg. Chem.* 2012, 51, 13289−13302

by the optically dilute method[42] using a degassed acetonitrile solution of $[Re(phen)(CO)_3(pyridine)](CF_3SO_3)$ (Φ_{em} = 0.18, λ_{ex} = 355 nm) as the standard solution.[43] Details on the MTT assays and ICP-MS have been reported previously.[26h]

Live-Cell Confocal Microscopy. HeLa cells in growth medium were seeded on a sterilized coverslip in a 60-mm tissue culture dish and grown at 37 °C under a 5% CO_2 atmosphere for 48 h. The culture medium was then removed and replaced with medium/DMSO (99:1 v/v) containing complex **3-PEG-NH$_2$** (10 μM) or **3-Et-NH$_2$** (10 μM). After incubation for 1 h, the medium was removed, and the cell layer was washed with PBS (1 mL × 3). The coverslip was mounted onto a sterilized glass slide and then imaged using a Leica TCS SPE confocal microscope. In the mitochondria-colocalization experiments, HeLa cells were treated with complex **3-PEG-NH$_2$** (10 μM) for 1 h and then incubated with MitoTracker Deep Red FM (100 nM) in FBS-free medium for 20 min, followed by washing with PBS (1 mL × 3). In the endosome-colocalization experiments, HeLa cells were incubated with complex **3-PEG-NH$_2$** (10 μM) and Alexa Fluor 633-conjugated transferrin (50 μg/mL) in medium for 1 h, followed by washing with PBS (1 mL × 3). The colocalization coefficients were determined by the program ImageJ (Version 1.4.3.67).

Lipophilicity (Log $P_{o/w}$). The lipophilicity of the complexes was determined using the flask-shaking method where *n*-octanol and an aqueous sodium chloride solution were used as the organic and aqueous phase, respectively. *n*-Octanol was presaturated with an aqueous solution of sodium chloride (0.9% w/v) by swirling at 45 rpm for 24 h. The complex was dissolved in the isolated organic phase at a concentration of 50 μM. An equal volume of aqueous sodium chloride solution (0.9% w/v) was added, and the mixture was swirled for 30 min at 45 rpm. The solution was then centrifuged, and the amounts of complex in both layers were determined by emission spectroscopy.

PEGylation of BSA with Complexes 1-PEG-NCS−4-PEG-NCS. The isothiocyanate complex (2.0 μmol) in anhydrous dimethylsulfoxide (DMSO, 50 μL) was added to BSA (13.0 mg, 0.2 μmol) in 50 mM carbonate buffer (450 μL) at pH 10. The mixture was stirred for 12 h in dark at room temperature. The solution was then diluted to 1.0 mL with 50 mM potassium phosphate buffer at pH 7.4 and loaded onto a PD-10 column equilibrated with the same buffer. The first elution band with yellow to orange emission was collected. Finally, the bioconjugates **1-PEG-BSA−4-PEG-BSA** were washed successively with potassium phosphate buffer using an YM-30 centricon, concentrated to 1.5 mL, and stored at 4 °C.

PEGylation of PEI with Complexes 1-PEG-NCS−4-PEG-NCS. The isothiocyanate complex (5.0 μmol) in anhydrous DMSO (50 μL) was added to PEI (12.5 mg, 0.5 μmol) in 50 mM carbonate buffer (450 μL) at pH 10. The mixture was stirred for 12 h in dark at room temperature. The solution was then diluted to 1.0 mL with 50 mM potassium phosphate buffer at pH 7.4 and loaded onto a PD-10 column equilibrated with the same buffer. The first elution band with yellow to orange emission was collected. Finally, conjugates **1-PEG-PEI−4-PEG-PEI** were washed successively with potassium phosphate buffer using an YM-30 centricon, concentrated to 1.5 mL, and stored at 4 °C.

Agarose Gel Electrophoresis Retardation Assays. Polyplexes composed of conjugate **3-PEG-PEI** (or unmodified PEI) and the pDNA pRL-TK with N/P ratios (the number of PEI nitrogen per DNA phosphate) from 1 to 32 were prepared by mixing different amounts of the PEI-PEG conjugate and pRL-TK in Tris-Cl buffer (50 mM, pH 7.4). After incubation for 30 min at room temperature, the polyplexes were analyzed by electrophoresis on a 0.9% (w/v) agarose gel containing ethidium bromide with Tris-acetate buffer at 100 V for 45 min. The gel was visualized using a Bio-Rad Gel Doc imager.

Zeta Potentials and Mean Hydrodynamic Diameter Measurements. Polyplexes composed of conjugate **3-PEG-PEI** (or unmodified PEI) and pRL-TK (4 μg) with N/P ratios from 1 to 32 in Tris-Cl buffer (80 μL, 50 mM, pH 7.4) were prepared and incubated for 30 min at room temperature. The mixture was then diluted 10-fold with the same buffer. The zeta potentials of the polyplexes were measured using Zetasizer Nano ZS (Malvern Instruments) with the following specifications: sampling time, 10−20 s; medium viscosity, 1.0031 cP; dielectric constant, 80.4; temperature, 20 °C; beam mode F(Ka) = 1.50 (Smoluchowsky). The particle size was determined with the following specifications: sampling time, 180 s; medium viscosity, 1.0031 cP; refractive index (RI) medium, 1.330; RI particle, 1.450; temperature, 20 °C. All the experiments were carried out in triplicate.

In Vitro Transfection (Luciferase Assays). HeLa cells were seeded at a density of 100,000 cells per dish in a 35 mm cell culture dish and incubated for 48 h at 37 °C under a 5% CO_2 atmosphere. The culture medium was replaced with DMEM (2 mL) containing 10% FBS 2 h prior to the transfection. The transfection experiments were performed with pRL-TK (4 μg). At the time of transfection, the medium was replaced with Opti-MEM (2 mL). Polyplexes composed of conjugate **3-PEG-PEI** (or unmodified PEI) and pRL-TK with different N/P ratios were incubated with the cells for 5 h. The medium was replaced with fresh growth medium (3 mL), and the cells were further incubated for 43 h. The polyplex Lipofectamine/pRL-TK and the naked pDNA were used as a positive and negative control, respectively. After incubation, the cells were permeabilized with cell lysis buffer (200 μL) (Promega) with one freeze−thaw cycle. The luciferase activity in the cell lysate was measured using a Luciferase Assay Kit (Promega) on a microplate reader (BMG FLUOstar OPTIMA). All the experiments were carried out in triplicate.

In Vivo Toxicity. To determine the 50% lethal concentration (LD_{50}), selected 4-hpf zebrafish (*Danio rerio*) embryos were exposed to complex **3-PEG-NH$_2$** and **3-Et-NH$_2$**, respectively, at a series of concentrations (0.3125, 0.625, 1.25, 2.5, 5, 10, 20, and 40 μM) dispersed in filtered tap water (pH 7, 28.5 °C) with Instant Ocean (60 ng/mL). DMSO was used as a carrier solvent for the complex in the embryo medium. The final concentration of DMSO in the treatment medium was 1% (v/v), a concentration which was determined to be nontoxic to zebrafish embryos.[44] Three replicates were set up for each concentration, including the control experiments in which no complex was present; each replicate consisted of 20 embryos exposed to 6 mL of testing medium in a Petri dish (diameter = 55 mm). Exposure to the complexes lasted from 4 to 120 hpf. Mortality of the embryos was monitored at five time points: 24, 48, 72, 96, and 120 hpf. The LD_{50} values were determined from the dependence of the mortality on the concentration of the complexes.

Fluorescence Imaging of Zebrafish Embryos. Selected 4-hpf zebrafish embryos were exposed to complex **3-PEG-NH$_2$** (20 μM) in filtered tap water (pH 7, 28.5 °C) with Instant Ocean (60 ng/mL). After incubation for 20 h, the medium was removed, and the embryos were washed twice thoroughly with deionized water. The embryos were then transferred to 6 mL of testing medium with 0.016 M tricaine for anesthetization and imaged using a fluorescence microscope (Olympus SZX 12) equipped with a mercury lamp (EXFO X-cite 120Q) as the excitation source.

■ ASSOCIATED CONTENT

Ⓢ Supporting Information

Characterization and electronic absorption spectral data of the rhenium(I) polypyridine complexes, MALDI-TOF mass spectra of the ligands py-PEG-NH$_2$ and bpy-PEG and complexes **1-PEG-NH$_2$−4-PEG-NH$_2$**, and emission spectrum of complex **2-PEG-NH$_2$** in butyronitrile glass at 77 K. This material is available free of charge via the Internet at http://pubs.acs.org.

■ AUTHOR INFORMATION

Corresponding Author

*E-mail: bhcheng@cityu.edu.hk (S.H.C.), bhkenlo@cityu.edu.hk (K.K.-W.L.). Fax: (+852) 3442 0522. Tel: (+852) 3442 7231.

Notes

The authors declare no competing financial interest.

■ ACKNOWLEDGMENTS

We thank the Hong Kong Research Grants Councils (Project No. CityU 102410) and the City University of Hong Kong (Project No. 7008174) for financial support. A.W.-T.C., M.-W.L., and S.P.-Y.L. acknowledge the receipt of a Postgraduate Studentship, a Research Tuition Scholarship, and an Outstanding Academic Performance Award administered by the City University of Hong Kong.

■ REFERENCES

(1) Veronese, F. M.; Pasut, G. *Drug Discovery Today* **2005**, *10*, 1451−1458.
(2) (a) Harris, J. M.; Martin, N. E.; Modi, M. *Clin. Pharmacokinet.* **2001**, *40*, 539−551. (b) Michaelis, M.; Cinatl, J.; Pouckova, P.; Langer, K.; Kreuter, J.; Matousek, J. *Anti-Cancer Drugs* **2002**, *13*, 149−154. (c) Mok, H.; Palmer, D. J.; Ng, P.; Barry, M. A. *Mol. Ther.* **2005**, *11*, 66−79. (d) Pai, S. S.; Przybycien, T. M.; Tilton, R. D. *AAPS J.* **2009**, *11*, 88−98. (e) Knop, K.; Hoogenboom, R.; Fischer, D.; Schubert, U. S. *Angew. Chem., Int. Ed.* **2010**, *49*, 6288−6308.
(3) (a) Veronese, F. M.; Saccà, B.; Polverino de Laureto, P.; Sergi, M.; Caliceti, P.; Schiavon, O.; Orsolini, P. *Bioconjugate Chem.* **2001**, *12*, 62−70. (b) Manta, C.; Ferraz, N.; Betancor, L.; Antunes, G.; Batista-Viera, F.; Carlsson, J.; Caldwell, K. *Enzyme Microb. Technol.* **2003**, *33*, 890−898. (c) Ozyilmaz, G. *J. Mol. Catal. B: Enzym.* **2009**, *56*, 231−236.
(4) Fujii, N.; Jacobsen, R. B.; Wood, N. L.; Schoeniger, J. S.; Guy, R. K. *Bioorg. Med. Chem. Lett.* **2004**, *14*, 427−429.
(5) (a) Duncan, R. *Nat. Rev. Drug Discovery* **2003**, *2*, 347−360. (b) Thompson, M. S.; Vadala, T. P.; Vadala, M. L.; Lin, Y.; Riffle, J. S. *Polymer* **2008**, *49*, 345−373.
(6) (a) Pendri, A.; Martinez, A.; Xia, J.; Shorr, R. G. L.; Greenwald, R. B. *Bioconjugate Chem.* **1995**, *6*, 596−598. (b) Mueller, C.; Capelle, M. A. H.; Arvinte, T.; Seyrek, E.; Borchard, G. *J. Pharm. Sci.* **2011**, *100*, 1648−1662.
(7) (a) Viht, K.; Padari, K.; Raidaru, G.; Subbi, J.; Tammiste, I.; Pooga, M.; Uri, A. *Bioorg. Med. Chem. Lett.* **2003**, *13*, 3035−3039. (b) Erbas, S.; Gorgulu, A.; Kocakusakogullari, M.; Akkaya, E. U. *Chem. Commun.* **2009**, 4956−4958.
(8) (a) Rapozzi, V.; Cogoi, S.; Spessotto, P.; Risso, A.; Bonora, G. M.; Quadrifoglio, F.; Xodo, L. E. *Biochemistry* **2002**, *41*, 502−510. (b) Rakestraw, J. A.; Baskaran, A. R.; Wittrup, K. D. *Biotechnol. Prog.* **2006**, *22*, 1200−1208.
(9) (a) Corma, A.; Garcìa, H.; Leyva, A. *J. Catal.* **2006**, *240*, 87−99. (b) Samanta, D.; Kratz, K.; Zhang, X.; Emrick, T. *Macromolecules* **2008**, *41*, 530−532.
(10) (a) Marin, V.; Holder, E.; Meier, M. A. R.; Hoogenboom, R.; Schubert, U. S. *Macromol. Rapid Commun.* **2004**, *25*, 793−798. (b) Holder, E.; Marin, V.; Meier, M. A. R.; Schubert, U. S. *Macromol. Rapid Commun.* **2004**, *25*, 1491−1496.
(11) (a) Yokoyama, M.; Okano, T.; Sakural, Y.; Suwa, S.; Kataoka, K. *J. Controlled Release* **1996**, *39*, 351−356. (b) Nishiyama, N.; Yokoyama, M.; Aoyagi, T.; Okano, T.; Sakurai, Y.; Kataoka, K. *Langmuir* **1999**, *15*, 377−383. (c) Iinuma, H.; Maruyama, K.; Okinaga, K.; Sasaki, K.; Sekine, T.; Ishida, S.; Ogiwara, N.; Johkura, K.; Yonemura, Y. *Int. J. Cancer* **2002**, *99*, 130−137. (d) Aronov, O.; Horowitz, A. T.; Gabizon, A.; Fuertes, M. A.; Perez, J. M.; Gibson, D. *Bioconjugate Chem.* **2004**, *15*, 814−823. (e) Garmann, D.; Warnecke, A.; Kalayda, G. V.; Kratz, F.; Jaehde, U. *J. Controlled Release* **2008**, *131*, 100−106.
(12) Che, C.-M.; Zhang, J.-L.; Lin, L.-R. *Chem. Commun.* **2002**, 2556−2557.
(13) Heldt, J.-M.; Fischer-Durand, N.; Salmain, M.; Vessières, A.; Jaouen, G. *J. Organomet. Chem.* **2004**, *689*, 4775−4782.
(14) Viola-Villegas, N.; Rabideau, A. E.; Cesnavicious, J.; Zubieta, J.; Doyle, R. P. *ChemMedChem* **2008**, *3*, 1387−1394.
(15) Li, S. P.-Y.; Liu, H.-W.; Zhang, K. Y.; Lo, K. K.-W. *Chem.—Eur. J.* **2010**, *16*, 8329−8339.
(16) (a) Wrighton, M. S.; Morse, D. L. *J. Am. Chem. Soc.* **1974**, *96*, 998−1003. (b) Fredericks, S. M.; Luong, J. C.; Wrighton, M. S. *J. Am. Chem. Soc.* **1979**, *101*, 7415−7417.
(17) (a) Connick, W. B.; Di Bilio, A. J.; Hill, M. G.; Winkler, J. R.; Gray, H. B. *Inorg. Chim. Acta* **1995**, *240*, 169−173. (b) Wenger, O. S.; Henling, L. M.; Day, M. W.; Winkler, J. R.; Gray, H. B. *Inorg. Chem.* **2004**, *43*, 2043−2048.
(18) (a) Yam, V. W.-W.; Lau, V. C.-Y.; Wu, L.-X. *J. Chem. Soc., Dalton Trans.* **1998**, 1461−1468. (b) Lam, S. C.-F.; Yam, V. W.-W.; Wong, K. M.-C.; Cheng, E. C.-C.; Zhu, N. *Organometallics* **2005**, *24*, 4298−4305.
(19) (a) Guo, X.-Q.; Castellano, F. N.; Li, L.; Szmacinski, H.; Lakowicz, J. R.; Sipior, J. *Anal. Biochem.* **1997**, *254*, 179−186. (b) Guo, X.-Q.; Castellano, F. N.; Li, L.; Lakowicz, J. R. *Anal. Chem.* **1998**, *70*, 632−637. (c) Shen, Y.; Maliwal, B. P.; Lakowicz, J. R. *J. Fluoresc.* **2001**, *11*, 315−318. (d) Kuśba, J.; Li, L.; Gryczynski, I.; Piszczek, G.; Johnson, M.; Lakowicz, J. R. *Biophys. J.* **2002**, *82*, 1358−1372.
(20) (a) Busby, M.; Gabrielsson, A.; Matousek, P.; Towrie, M.; Di Bilio, A. J.; Gray, H. B.; Vlček, A., Jr. *Inorg. Chem.* **2004**, *43*, 4994−5002. (b) Gabrielsson, A.; Matousek, P.; Towrie, M.; Hartl, F.; Záli, S.; Vlček, A., Jr. *J. Phys. Chem. A* **2005**, *109*, 6147−6153. (c) Blanco-Rodrkguez, A. M.; Busby, M.; Grdinaru, C.; Crane, B. R.; Di Bilio, A. J.; Matousek, P.; Towrie, M.; Leigh, B. S.; Richards, J. H.; Vlček, A., Jr.; Gray, H. B. *J. Am. Chem. Soc.* **2006**, *128*, 4365−4370.
(21) (a) Wallace, L.; Rillema, D. P. *Inorg. Chem.* **1993**, *32*, 3836−3843. (b) Villegas, J. M.; Stoyanov, S. R.; Huang, W.; Rillema, D. P. *Dalton Trans.* **2005**, 1042−1051.
(22) (a) Zipp, A. P.; Sacksteder, L.; Streich, J.; Cook, A.; Demas, J. N.; DeGraff, B. A. *Inorg. Chem.* **1993**, *32*, 5629−5632. (b) Sacksteder, L.; Lee, M.; Demas, J. N.; DeGraff, B. A. *J. Am. Chem. Soc.* **1993**, *115*, 8230−8238. (c) Kneas, K. A.; Xu, W.; Demas, J. N.; Zipp, B. A.; DeGraff, A. P. *J. Fluoresc.* **1998**, *8*, 295−300.
(23) Smithback, J. L.; Helms, J. B.; Schutte, E.; Woessner, S. M.; Sullivan, B. P. *Inorg. Chem.* **2006**, *45*, 2163−2174.
(24) (a) Lees, A. J. *Chem. Rev.* **1987**, *87*, 711−743. (b) Kotch, T. G.; Lees, A. J.; Fuerniss, S. J.; Papathomas, K. I. *Chem. Mater.* **1991**, *3*, 25−27. (c) Kotch, T. G.; Lees, A. J.; Fuerniss, S. J.; Papathomas, K. I. *Chem. Mater.* **1992**, *4*, 675−683. (d) Kotch, T. G.; Lees, A. J.; Fuerniss, S. J.; Papathomas, K. I.; Snyder, R. W. *Inorg. Chem.* **1993**, *32*, 2570−2575. (e) Sun, S.-S.; Lees, A. J. *Organometallics* **2002**, *21*, 39−49.
(25) Stephenson, K. A.; Banerjee, S. R.; Besanger, T.; Sogbein, O. O.; Levadala, M. K.; McFarlane, N.; Lemon, J. A.; Boreham, D. R.; Maresca, K. P.; Brennan, J. D.; Babich, J. W.; Zubieta, J.; Valliant, J. F. *J. Am. Chem. Soc.* **2004**, *126*, 8598−8599.
(26) (a) Lo, K. K.-W.; Ng, D. C.-M.; Hui, W.-K.; Cheung, K.-K. *J. Chem. Soc., Dalton Trans.* **2001**, 2634−2640. (b) Lo, K. K.-W.; Hui, W.-K.; Ng, D. C.-M.; Cheung, K.-K. *Inorg. Chem.* **2002**, *41*, 40−46. (c) Lo, K. K.-W.; Hui, W.-K.; Ng, D. C.-M. *J. Am. Chem. Soc.* **2002**, *124*, 9344−9345. (d) Lo, K. K.-W.; Tsang, K. H.-K.; Hui, W.-K.; Zhu, N. *Chem. Commun.* **2003**, *21*, 2704−2705. (e) Lo, K. K.-W.; Tsang, K. H.-K.; Sze, K.-S. *Inorg. Chem.* **2006**, *45*, 1714−1722. (f) Lo, K. K.-W.; Tsang, K. H.-K.; Zhu, N. *Organometallics* **2006**, *25*, 3220−3227. (g) Lo, K. K.-W.; Sze, K.-S.; Tsang, K. H.-K.; Zhu, N. *Organometallics* **2007**, *26*, 3440−3447. (h) Louie, M.-W.; Lui, H.-W.; Lam, M. H.-C.; Lau, T.-C.; Lo, K. K.-W. *Organometallics* **2009**, *28*, 4297−4307. (i) Louie, M.-W.; Liu, H.-W.; Lam, M. H.-C.; Lam, Y.-W.; Lo, K. K.-W. *Chem.—Eur. J.* **2011**, *17*, 8304−8308. (j) Louie, M.-W.; Fong, T. T.-H.; Lo, K. K.-W. *Inorg. Chem.* **2011**, *50*, 9465−9471.
(27) (a) Reitz, G. A.; Demas, J. N.; DeGraff, B. A.; Stephens, E. M. *J. Am. Chem. Soc.* **1988**, *110*, 5051−5059. (b) Coogan, M. P.; Fernández-Moreira, V.; Hess, J. B.; Pope, S. J. A.; Williams, C. *New J. Chem.* **2009**, *33*, 1094−1099.
(28) (a) Bailon, P.; Berthold, W. *Pharm. Sci. Technol. Today* **1998**, *1*, 352−356. (b) Harris, J. M.; Chess, R. B. *Nat. Rev. Drug. Discovery* **2003**, *2*, 214−221.
(29) (a) Lo, K. K.-W.; Ng, D. C.-M.; Chung, C.-K. *Organometallics* **2001**, *20*, 4999−5001. (b) Lo, K. K.-W.; Chung, C.-K.; Lee, T. K.-M.; Lui, L.-H.; Tsang, K. H.-K.; Zhu, N. *Inorg. Chem.* **2003**, *42*, 6886−6897. (c) Lo, K. K.-W.; Chan, J. S.-W.; Chung, C.-K.; Tsang, V. W.-H.; Zhu, N. *Inorg. Chim. Acta* **2004**, *357*, 3109−3118. (d) Leung, S.-K.;

Kwok, K. Y.; Zhang, K. Y.; Lo, K. K.-W. *Inorg. Chem.* **2010**, *49*, 4984−4995. (e) Lee, P.-K.; Liu, H.-W.; Yiu, S.-M.; Louie, M.-W.; Lo, K. K.-W. *Dalton Trans.* **2011**, *40*, 2180−2189.
(30) (a) Boussif, O.; Lezoualc'h, F.; Zanta, M. A.; Mergny, M. D.; Scherman, D.; Demeneix, B.; Behr, J. P. *Proc. Natl. Acad. Sci. U.S.A.* **1995**, *92*, 7297−7301. (b) Rudolph, C.; Lausier, J.; Naundorf, S.; Müller, R. H.; Rosenecker, J. *J. Gene Med.* **2000**, *2*, 269−278. (c) Akinc, A.; Thomas, M.; Klibanov, A. M.; Langer, R. *J. Gene Med.* **2004**, *7*, 657−663.
(31) (a) Bieber, T.; Meissner, W.; Kostin, W.; Niemann, A.; Elsasser, H.-P. *J. Controlled Release* **2002**, *82*, 441−454. (b) Grosse, S.; Aron, Y.; Thévenot, G.; Monsigny, M.; Fajac, I. *J. Controlled Release* **2007**, *122*, 111−117. (c) Sunoqrot, S.; Bae, J. W.; Jin, S.-E.; Pearson, R. M.; Liu, Y.; Hong, S. *Bioconjugate Chem.* **2011**, *22*, 466−474. (d) Louie, M.-W.; Choi, A. W.-T.; Liu, H.-W.; Chan, B. T.-N.; Lo, K. K.-W. *Organometallics* **2012**, *31*, 5844−5855. (e) Li, S. P.-Y.; Tang, T. S.-M.; Yiu, K. S.-M.; Lo, K. K.-W. *Chem.—Eur. J.* **2012**, *18*, 13342−13354.
(32) (a) Erbacher, P.; Bettinger, T.; Belguise-Valladier, P.; Zou, S.; Coll, J.-L.; Behr, J.-P.; Remy, J.-S. *J. Gene Med.* **1999**, *1*, 210−222. (b) Nguyen, H.-K.; Lemieux, P.; Vinogradov, S. V.; Gebhart, C. L.; Guerin, N.; Paradis, G.; Bronich, T. K.; Alakhov, V. Y.; Kabanov, A. V. *Gene Ther.* **2000**, *7*, 126−138. (c) Vinogradov, S. V.; Bronich, T. K.; Kabanov, A. V. *Bioconjugate Chem.* **1998**, *9*, 805−812. (d) Petersen, H.; Fechner, P. M.; Martin, A. L.; Kunath, K.; Stolnik, S.; Roberts, C. J.; Fischer, D.; Davies, M. C.; Kissel, T. *Bioconjugate Chem.* **2002**, *13*, 845−854.
(33) Hyvönen, Z.; Plotniece, A.; Reine, I.; Chekavichus, B.; Dubur, G.; Urtti, A. *Biochim. Biophys. Acta* **2000**, *1509*, 451−466.
(34) Booth, D. T. *J. Exp. Biol.* **1995**, *198*, 241−247.
(35) Cheng, J.; Flahaut, E.; Cheng, S. H. *Environ. Toxicol. Chem.* **2007**, *26*, 708−716.
(36) Perrin, D. D.; Armarego, W. L. F. *Purification of Laboratory Chemicals*, 3rd ed.; Pergamon Press: New York, 1988.
(37) Lo, K. K.-W.; Louie, M.-W.; Sze, K.-S.; Lau, J. S.-Y. *Inorg. Chem.* **2008**, *47*, 602−611.
(38) Peek, B. M.; Ross, G. T.; Edwards, S. W.; Meyer, G. J.; Meyer, T. J.; Erickson, B. W. *Int. J. Pept. Protein Res.* **1991**, *38*, 114−123.
(39) Lo, K. K.-W.; Hui, W.-K. *Inorg. Chem.* **2005**, *44*, 1992−2002.
(40) Lo, K. K.-W.; Lee, T. K.-M.; Zhang, K. Y. *Inorg. Chim. Acta* **2006**, *359*, 1845−1854.
(41) Westerfield, M. *The Zebrafish Book: A Guide for the Laboratory Use of Zebrafish (Danio rerio)*; University of Oregon Press: Eugene, OR, 2007.
(42) Demas, J. N.; Crosby, G. A. *J. Phys. Chem.* **1971**, *75*, 991−1024.
(43) Wallace, L.; Rillema, D. P. *Inorg. Chem.* **1993**, *32*, 3836−3843.
(44) Lahnsteiner, F. *Theriogenology* **2008**, *69*, 384−396.